geologica acta

Citation: Hernaiz-Huerta, P.P., Ramos, A., Ardévol, Ll., 2026. The Muschelkalk (Middle Triassic) in the SE sector of Sierra del Espadán (Iberian Range, Spain). Geologica Acta, 24.1, 1-pgs. DOI: 10.1344/GeologicaActa2026.24.1 Online ISSN: 1696-5728

The Muschelkalk (Middle Triassic) in the SE sector of Sierra del Espadán (Iberian Range, Spain)

Pedro Pablo Hernaiz-Huerta[1] **Adrià Ramos**[2,3] **Lluis Ardévol**[4]

[1]**Centro Nacional Instituto Geologico y Minero de España (CN IGME-CSIC)**
c/ Rios Rosas 23, 28003, Madrid, Spain. E-mail: p.hernaiz@igme.es ORCID: 0000-0002-7961-5854

[2]**Departament de Botànica i Geologia, Universitat de València**
Av. Vicent Andrés Estellés, 19. 46100 Burjassot, València

[3]**Departament de Ciències de la Terra i del Medi Ambient, Universitat d'Alacant**
c/ San Vicente del Raspeig s/n, 03690 San Vicente del Raspeig, Alacant, Spain. E-mail: adria.ramos@uv.es ORCID: 0000-0001-8224-9165

[4]**Geoplay**
c/ Nerets 6, 25630, Talarn, Lleida, Spain. E-mail: lluis@geoplay.cat

ABSTRACT

Detailed mapping of the southeastern sector of the Sierra del Espadán (Eastern Iberian Range) shows that the Muschelkalk M2 intermediate unit is extensively distributed across the region, including its coastal areas. The M2 unit forms a thin (up to 25-30m), incompetent horizon predominantly composed of marly-dolomitic facies. Local stratigraphic omissions of this unit, resulting from facies changes or lateral wedging, occasionally led to continuous dolomitic successions corresponding to the Muschelkalk M1 plus the lower M3 (M3i) units. The M1 unit has been consistently mapped throughout the area, maintaining stratigraphic continuity with the underlying Röt facies, which cap the Buntsandstein B2 succession. Similar stratigraphic patterns have been observed in the adjacent Sierra Calderona to the South. These features collectively support the interpretation that both mountain ranges belong to the Mediterranean Triassic Domain, rather than to the Levantine–Balearic Domain. The Muschelkalk is transitionally overlain, by a previously undescribed, thick marly-clayey succession which includes thin, well-bedded dolostones—resembling those of the lower M3 (M3i) unit—and abundant packages of dolomitic breccias. This newly identified interval is herein provisionally interpreted as a possible stratigraphic unit, the "supra-Pina de Montalgrao" facies referring to its position overlying the uppermost Muschelkalk M3 (M3s) Pina de Montalgrao Formation, pending paleontological evidence to confirm its age. The dolomitic breccias are interpreted as the result of fragmentation of thin, well-bedded dolostones, possibly triggered by gravitational instabilities associated with late-stage reactivation of Permian–Triassic rifting. Nonetheless, a dissolution process involving stratigraphically related evaporitic deposits remains a plausible alternative origin for some of these breccias.

KEYWORDS **Muschelkalk. "Supra-Pina de Montalgrao" facies/unit. Dolomitic breccias. Sierra del Espadán. Iberian Range.**

INTRODUCTION

The break-up of the Pangaea at the end of the Palaeozoic, as a result of an intense and sustained rifting process, marks the beginning of the Alpine Cycle and the individualisation of the Iberian (micro)-plate in a peripheral position with respect to the western Tethys that was breaking through to the west (Gómez, 2019a; Sanchez Moya and Sopeña, 2004; Ziegler, 1982, 1988). As a result, Permo-Triassic rocks are abundant in the Iberian Peninsula with a preferential distribution around most of the Iberian (Variscan) Massif (Fig. 1).

Three main types of successions have been distinguished in the Triassic of the Iberian Peninsula on the basis of their facies and palaeogeographic conditions (López-Gómez *et al.*, 1998; Ortí *et al.*, 2017; Pérez-López and Pérez-Valera, 2007; Pérez-López *et al.* 2021; Sopeña *et al.*, 1988; Virgili *et al.*, 1977; among others): The Hesperian Triassic consists of a sequence of continental siliciclastic facies, deposited along the eastern margin of the Iberian Massif. The Epicontinental Triassic corresponds to the typical Germanic facies trilogy, composed of a lower continental siliciclastic Buntsandstein, a middle Muschelkalk consisting predominantly of shallow marine carbonate facies, and an upper Keuper primarily characterized by evaporitic deposits. Finally, the Alpine Triassic refers to predominantly marine carbonate facies extending up to the Upper Triassic that are relatively deeper and, in general, thicker than the previous ones. These facies are only found in the Internal Zones of the Betic Cordillera. Within the Epicontinental Triassic, two subdivisions are also recognized. A sector comprises the central-eastern part of the Iberian Range, the Catalan Coastal Range, and most of the Ebro Basin, where the Muschelkalk is represented by two main carbonate units, M1 and M3, separated by an intermediate interval (M2) of mixed siliciclastic-carbonate-evaporitic nature. This type of succession is referred to as the Mediterranean Triassic. In the other sector, referred to as the Iberian Triassic, the Muschelkalk is represented solely by the upper carbonate unit (M3) and is located to the west and south of the previous one.

In addition, López Gómez *et al.* (1998) suggested the designation of a third subdivision, the Levantine-Balearic Triassic, for those successions characterized by a continuous carbonate Muschelkalk unit (M1+M3) due to the disappearance (via facies change or thinning) of the intermediate M2 unit. This type of succession is typical of the Balearic Triassic and, according to López Gómez

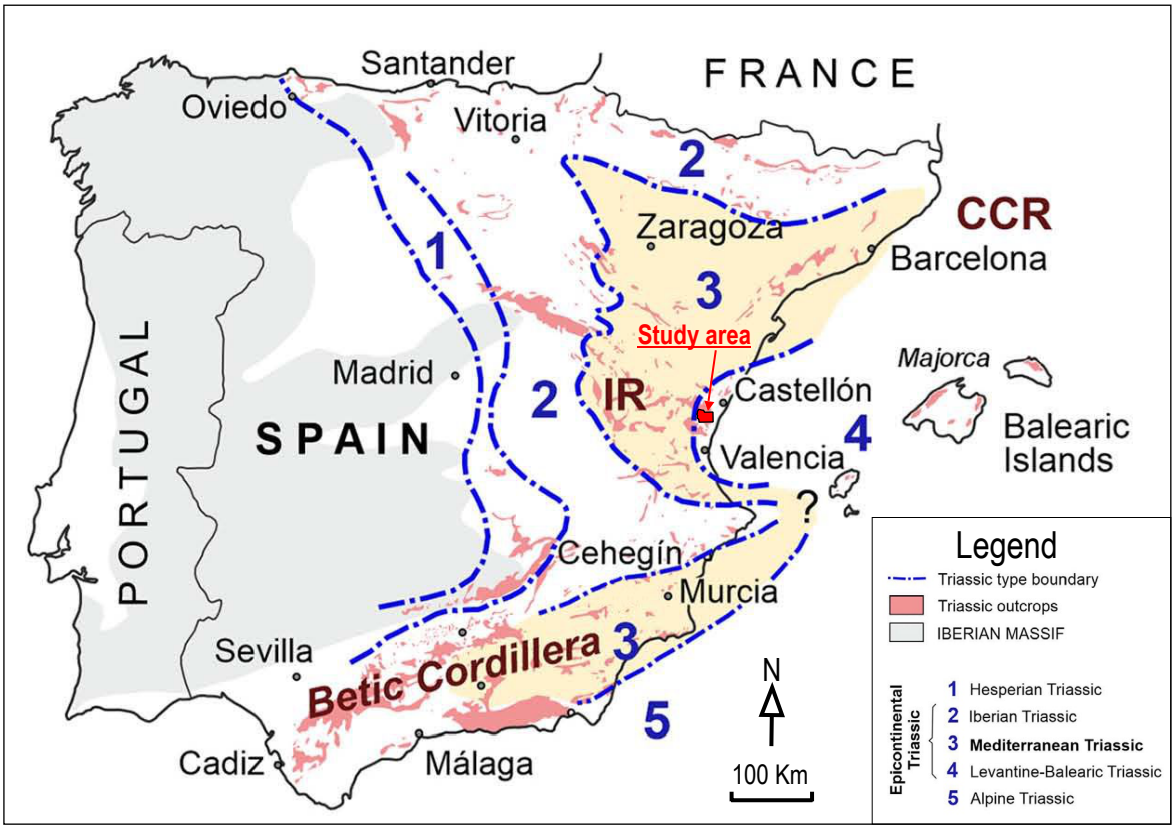

FIGURE 1. Distribution of outcrops and types of Triassic successions in Spain (following López-Gómez *et al.*, 1998 and adapted from Pérez-Valera *et al.*, 2023). The location of the study area is indicated (red square). IR: Iberian Range; CCR: Catalan Coastal Range.

et al. (1998), extends into the eastern areas of Valencia and Castellón provinces near the coast (Fig. 1). Escudero-Mozo *et al.* (2015) assumed the existence of the Levantine-Balearic Triassic in the easternmost part of the Iberian Range with a broader extent (farther west) than initially proposed by López-Gómez *et al.* (1998). Based on new paleontological and stratigraphic data, Escudero-Mozo *et al.* (2015) suggest that the entire Muschelkalk consists of a single carbonate unit, assigned to the M3, in the extended Levantine-Balearic Triassic.

In all of the Triassic successions, particularly in the Epicontinental Triassic, the switch from the shallow marine carbonate facies of the upper-most Muschelkalk to the eminently evaporitic or clastic-evaporitic facies of the Keuper, typical of restricted coastal environments, is systematically described as transitional (Escudero Mozo *et al.*, 2019 -fig. 3.34 therein-; Ortí and Pérez-López, 2019; Ortí *et al.*, 2017, 2022; Salvany, 1990). The Keuper facies expand over the underlying Muschelkalk and, generally, exhibit greater thickness variations than the latter, especially in the southwestern sector of the Iberian Range, in the subsurface of the Tabular Cover (Ortí and Pérez-López, 2019), and in the External Zones of the Betic Cordillera (Ortí *et al.*, 2017; Pérez-López and Pérez-Valera, 2007; Pérez-López *et al.*, 2019). These greater thickness variations in the Keuper are attributed to late reactivations during the terminal phase of the Permo-Triassic mechanical stretching, prior to the onset of the subsequent thermal subsidence stage (Ortí and Pérez-López, 2019; Pérez-López and Pérez-Valera, 2021). This latter stage is marked by the widespread, regional establisment of an extensive shallow carbonate platform represented by the Imón Formation (and equivalents) of Norian-Rhaetian age (Gómez, 2019b). However, descriptions of lithologies that could be interpreted as tectofacies associated with these reactivations are scarce in both the Keuper and the underlying Muschelkalk (Pérez-López and Pérez-Valera, 2021).

The Levantine sector of the Castillian Branch of the Iberian Range, which includes the Triassic domains of Sierras del Espadán and Calderona (Fig. 1), is a key area for studying some of the Triassic successions described above, specifically the Mediterranean and Levantine-Balearic types. The geological maps of this sector, executed during the early stages of the Spanish Geological Mapping Programme (Plan MAGNA) in the 1970s, barely incorporate the updated stratigraphic framework of the Triassic and Jurassic. Consequently, both the stratigraphic and structural interpretations require revision in light of modern concepts such as extensional tectonics, tectonic inversion, thrust tectonics, and even salt tectonics. Furthermore, the mapping of these domains is significantly challenging due to the notable convergence of facies between the different carbonate (*e.g.* M1, M3, Imón Fm) and siliciclastic-carbonate-evaporitic (*e.g.* M2 and Keuper) units, further compounded by a complex tectonic history.

A significant portion of the Sierra Calderona and the southwestern sector of the Sierra del Espadán including the environ of La Vall d'Uixó town, have recently been mapped as part of a 1:25,000 scale geological mapping project undertaken by the CN IGME_CSIC in collaboration with the Institut Cartogràfic Valencià (ICV). This mapping project aims to provide comprehensive geological coverage of the coastal region belonging to the Comunitat Valenciana. The present work describes the results obtained in the mapping of the Muschelkalk M2 and, mainly, M3 units of the La Vall d'Uixó sheet (No. 668-II), and its extension towards the W and NW up to the surroundings of the villages of Azuébar and Chóvar. The level of detail required by the new mapping scale has revealed significant stratigraphic peculiarities within these units. Field observations have been complemented by the logging of key lithostratigraphic sections.

The aims of this study are i) to assess the occurrence and continuity of an eminently marly-clayey M2 unit in the area, extending all the way to the coast, between the carbonate M1 and M3 units; ii) to investigate the distinctive nature of the transition between the M3 and the Keuper in the region; and iii) discuss the implications of the occurrence of these stratigraphic units on the paleogeographic interpretations of the western Tethys.

GEOLOGICAL FRAMEWORK

The Palancia River depression marks the boundary between the Sierra del Espadán and the neighbouring Sierra Calderona to the South. Together, these mountain ranges define the southeastern termination of the Levantine Sector within the Castilian Branch of the Iberian Cordillera, adjacent to the Valencian coastal margin. They represent distinct geological domains, predominantly composed of classical Permo-Triassic stratigraphic units, including the Buntsandstein, Muschelkalk and Keuper facies. These units are partially overlain by a Jurassic cover, predominantly comprising Lower Jurassic formations with more limited representation of Middle and Upper Jurassic formations (Fig. 2).

The geodynamic evolution of the Sierra del Espadán and Sierra Calderona is entirely governed by the Alpine Cycle, which is chronologically expressed in the region through three main tectonic phases: i) Permo-Triassic extension associated with the development of the so-called (Triassic) Iberian Basin (De la Horra *et al.*, 2019; Gómez, 2019; Sánchez Moya and Sopeña, 2004), with no evidence

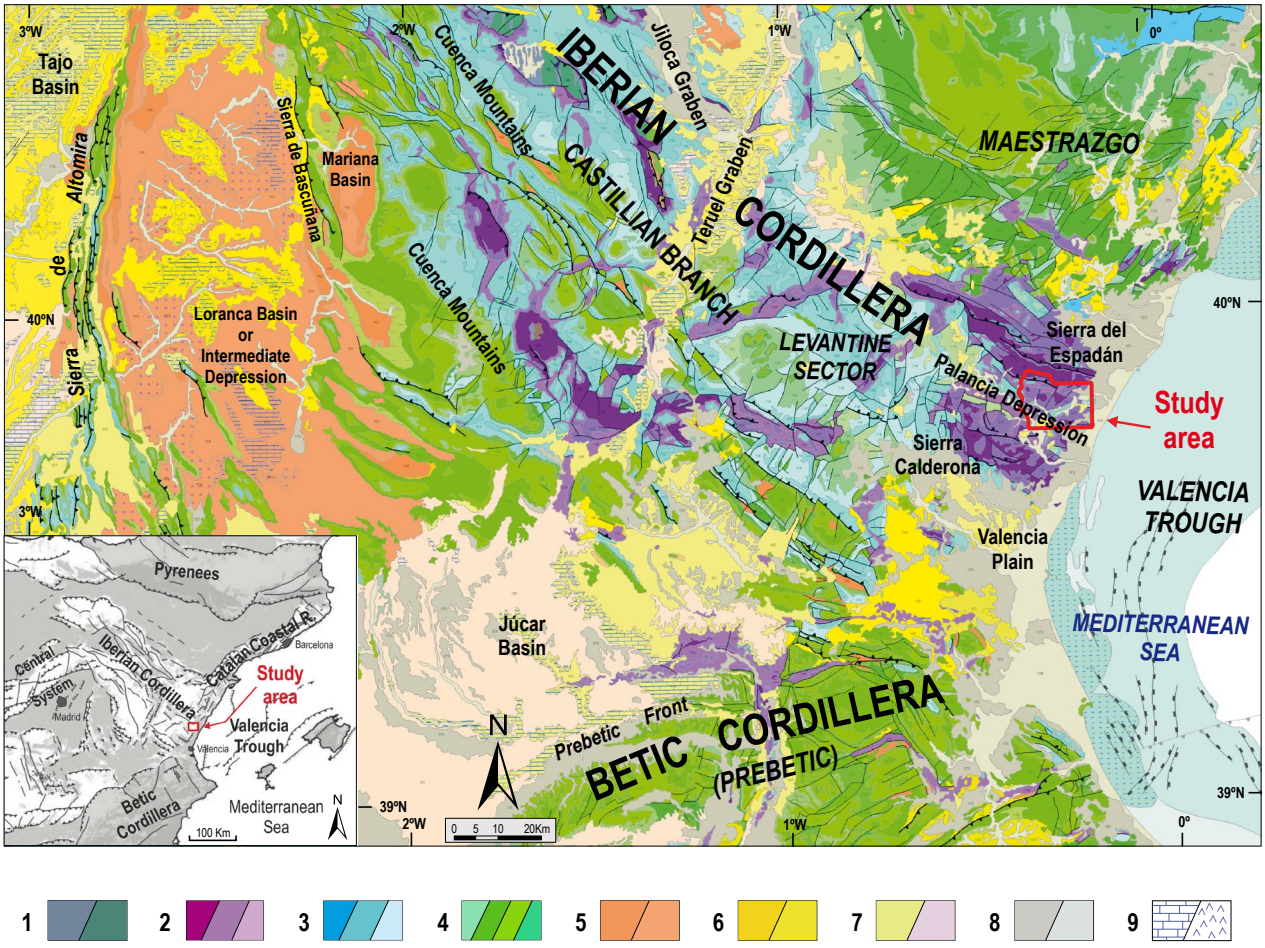

FIGURE 2. Geological framework of the study area (adapted and modified from IGME/LNEG (2015)). 1. Paleozoic; 2. Permian-Triassic; 3. Jurassic; 4. Cretaceous; 5. Paleogene; 6. Miocene; 7. Pliocene; 8. Quaternary; 9. Limestones/Gypsum. Modified from Hernaiz Huerta (2024a).

in the study area of the subsequent Upper Jurassic-Lower Cretaceous extension phase due to the absence of related deposits (Liesa *et al.*, 2019); ii) late Eocene-Oligocene to lower Miocene compressional deformation related to the Alpine construction of the Iberian Cordillera (Álvaro *et al.*, 1979; De Vicente *et al.*, 2009, 2019; Guimerá and Álvaro, 1990) and iii) Neogene extension associated with the opening of the Valencia Trough (Fontboté *et al.*, 1990; Simón, 2004; Vegas, 1992).

The general, contractional structure of these sierras responds to thick-skinned tectonics. This is characterised by long-wave length folds with a typically Iberian (Range) NW-SE to WNW-ESE direction, associated with thrusts and reverse faults that involve the tectonic basement formed by the Palaeozoic and the structurally coupled Permo-Triassic units (Hernaiz Huerta, 2022, 2024a; Ortí *et al.*, 2020). The Jurassic overlying cover, where preserved, is interpreted as being primarily detached along the Keuper horizon and folded disharmonically relative to the basement, sometimes with internal imbrications. In contrast to Sierra Calderona, where the structure is essentially anticlinorial, in Sierra del Espadán some thrusts expose the Palaeozoic basement partially overriding the Permo-Triassic units.

Close to the coast, the dominant contractional structure in both mountain ranges is significantly distorted by Neogene extensional tectonics associated with the opening of the Valencia Trough (Hernaiz Huerta, 2022, 2024a, c). This is primarily manifested as a pronounced network of normal faults subparallel to the coast, which control the sinking of blocks in the same direction. It is also common to identify Iberian-oriented normal faults coeval with these ones.

Figure 3 shows the geological map of the surveyed area and its legend. The quartzitic sandstones of the Buntsandstein B1 and the alternation of micaceous sandstones and red siliciclastic mudstones of the Buntsandstein B2 occupy the cores of the Iberian-oriented anticlines, which appear

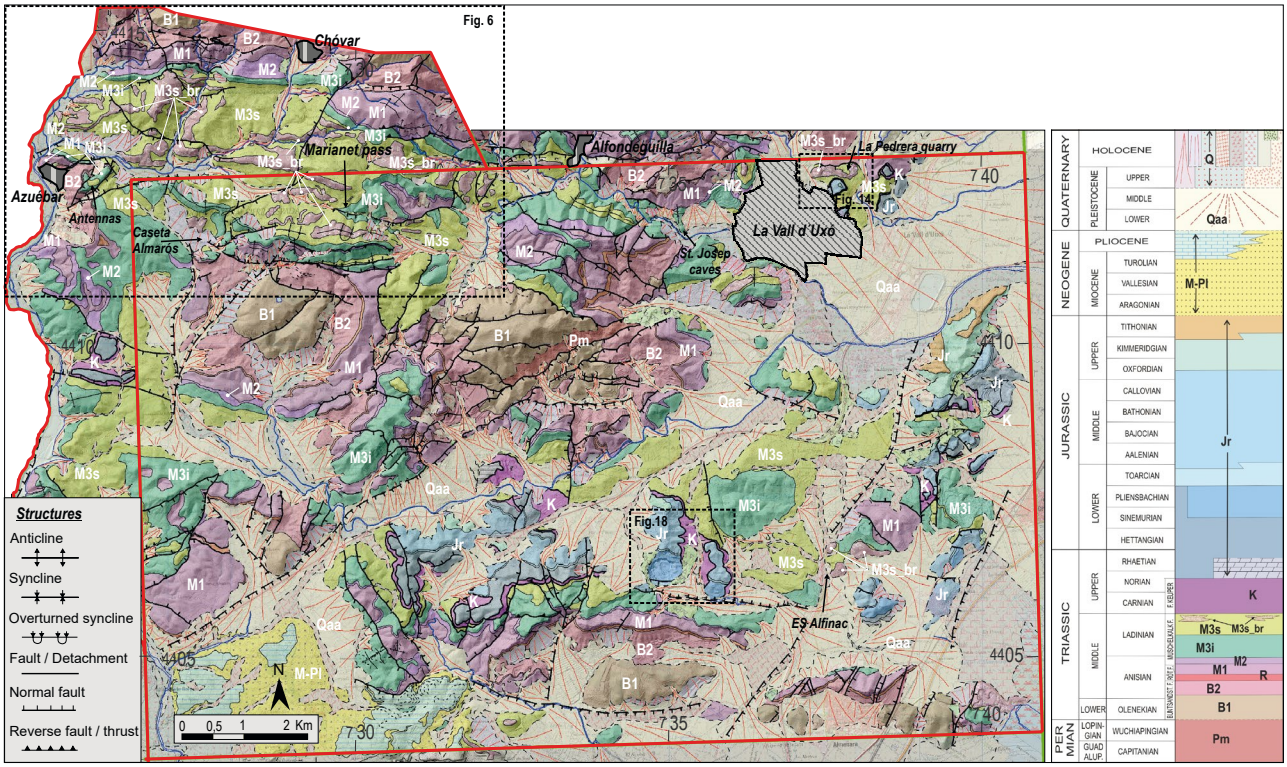

FIGURE 3. Geological map and general stratigraphy of the study area, adapted and extended from Hernaiz-Huerta (2023, 2024b). The red line marks the boundaries of the 1:25,000 scale Vall d'Uixó sheet and the expanded area reaching the vicinity of Azuébar (to the West) and Chóvar (to the North) villages. Dashed black rectangles show the situation of Figures 6, 14 and 18. Localities and toponymical references cited in the text are shown in black. The initials used in the legend and on the map for the geological units or formations are those used in the text. Pm: Permian; B1: Buntsandstein B1; B2: Buntsandstein B2; R: Röt; M1: Muschelkalk M1; M2: Muschelkalk M2; M3i: Lower Muschelkalk M3; M3s: Upper Muschelkalk M3; M3s_br: Thin, well-bedded dolostones and dolomitic breccias; K: Keuper; Jr: Undifferentiated Jurassic; M-Pl: Miocene-Pliocene; Qaa: Pleistocene alluvial fans; Q: Undifferentiated Quaternary (see explanation in the text).

highly distorted and misaligned due to the effect of NE-SW to NNE-SSW oriented normal faults associated with the Neogene extension. In the central anticline, one of these faults allows the outcrop of quartzitic sandstones alternating with reddish wine-coloured siltstones and claystones that belong to the Permian (Pm) and underlie the Buntsandstein B1. The flanks of the anticlines and the cores of the linking synclines between them are formed by the carbonate or marl-carbonate units of the Muschelkalk (M1, M2 and M3). The Jurassic succession (Jr) outcrops relatively complete (up to the Tithonian) but discontinuous in the two eastern blocks, as well as in several isolated fragments scattered throughout the rest of the study area, in this case exclusively comprising its basal terms (Lower Jurassic). The Keuper (Kp) is usually recognized forming discontinuous patches at its base.

Clastic and marly continental deposits, presumably belonging to the Miocene-Pliocene (M-Pl), which transition upwards into massive or broadly bedded limestones, with gastropods, of Late Miocene-Pliocene age, complete the stratigraphy of the surveyed area. Additionally, there is an extensive network of alluvial fans (Qaa) attributable to the Pleistocene, along with other minor Quaternary deposits (Q).

METHODS

This study is the outcome of comprehensive geological mapping and the field observations made during its execution. The mapping employed a combination of traditional and modern techniques. Bedding and other structural data were recorded with georeferencing using FieldMOVE software (PE Limited) on a 6th generation iPad, and imported into ArcMap within the ArcGIS suite. All principal contacts and faults were delineated in the field using stereoscopic vision on high-quality, high-resolution 1:30,000 scale aerial photographs from 1986. The final digital map was produced with ArcMap, incorporating orthophotos and, in less accessible areas, 3D visualization from Google Earth. The map was overlaid on a 1:25,000 topographic base enhanced with a Digital Terrain Model/Height Surface (DTM/HS) background, both provided by Spanish Geographic Institute (IGN). The entire mapping process adhered to the internal guidelines specific to the project, established by the CN IGME_CSIC in collaboration

with the ICV. Some key lithostratigraphic sections were logged using Jacob´s staff and studied under sedimentary field standards. MOVE software (PE Limited) was used to draw the geological cross-sections.

GENERAL STRATIGRAPHY AND RESEARCH BACKGROUND OF THE MUSCHELKALK IN THE STUDY AREA

The nomenclature of Garay (2001) is followed for the Permo-Triassic units in the study region. The equivalences between the Permo-Triassic units and formations used here and those proposed by other authors are shown in Figure 4. The stratigraphic details of the Permo-Triassic units other than the Muschelkalk, as well as those of the Jurassic or Tertiary, are beyond the scope of this work.

The lower carbonate unit of the Muschelkalk (M1) is the L'Oronet Fm (Garay, 2001). It overlies the red mudstones and sandstones of the Buntsandstein Serra Fm (B2) through a transitional Röt facies unit which is characterized by alternating red and green/grey laminated siltstones, claystones, and marls, with centimetre-scale intercalations of fine-grained sands and yellowish carbonates. This interval was designated by Garay (2001) as the Olocau Variegated Member of the Serra Fm (labelled –R- in Figs. 3; 5; 6; Fig. 4). With an average thickness of about 20-35m it has a persistent occurrence in the region as a reference level below the L'Oronet Fm although its lithology favours its local detachment. The L'Oronet Fm consists of thick (30-50cm) and thin (10-20cm) well-bedded dolostones and limestones locally alternating with marls, which show dominant brown and dark ochre tones (Fig. 5A, B). The average thickness is around 100m.

The Azuébar Fm (Garay, 2001) corresponds to the low competent interval of the Muschelkalk (M2), clearly sandwiched between the carbonate M1 and M3 units. Its thickness in the study area ranges between 10 and 30-

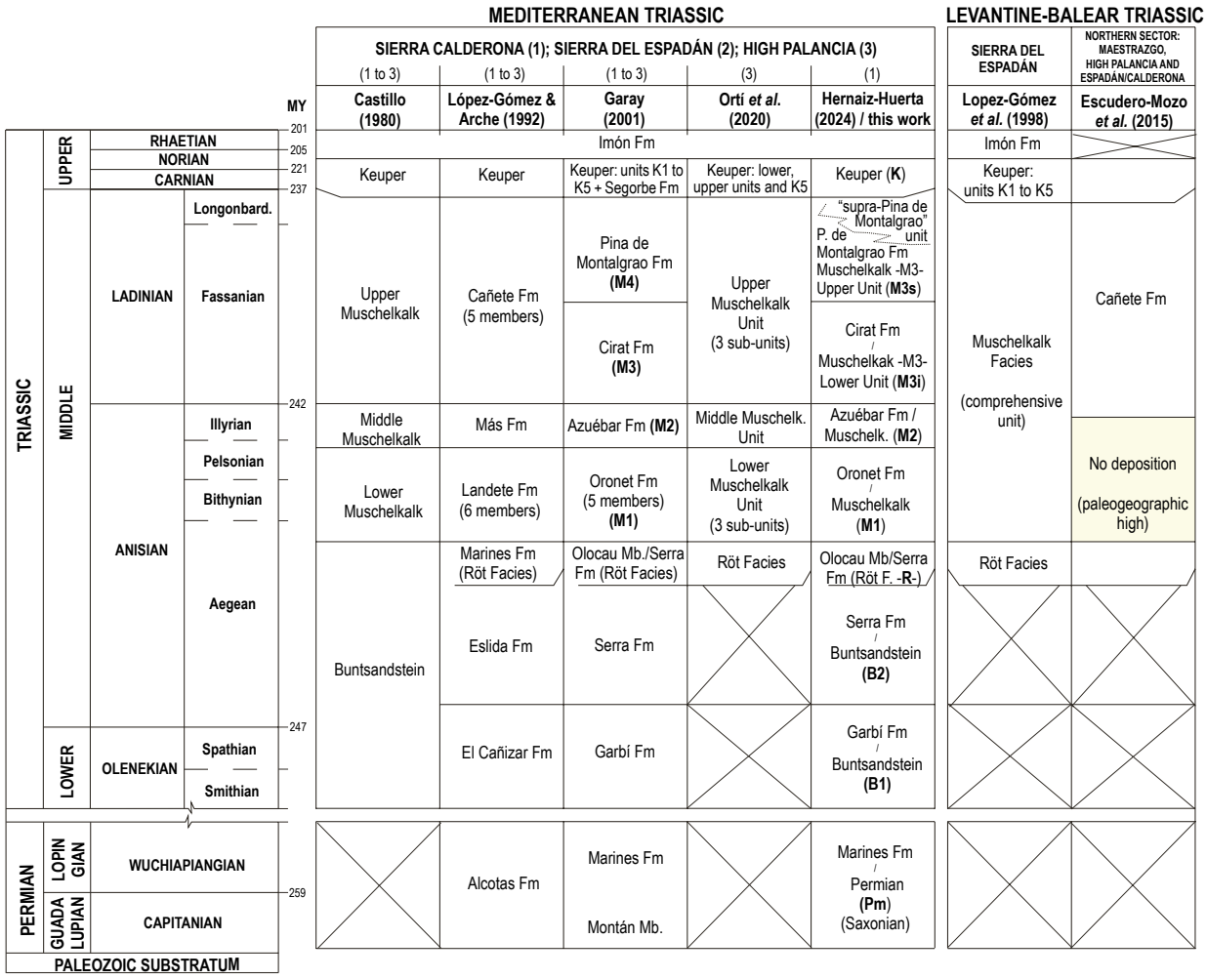

FIGURE 4. Comparative framework of Permo-Triassic stratigraphic units proposed by different authors in the eastern sector of the Iberian Cordillera. Adapted and modified from Ortí *et al.* (2020) and Hernaiz-Huerta, 2024.

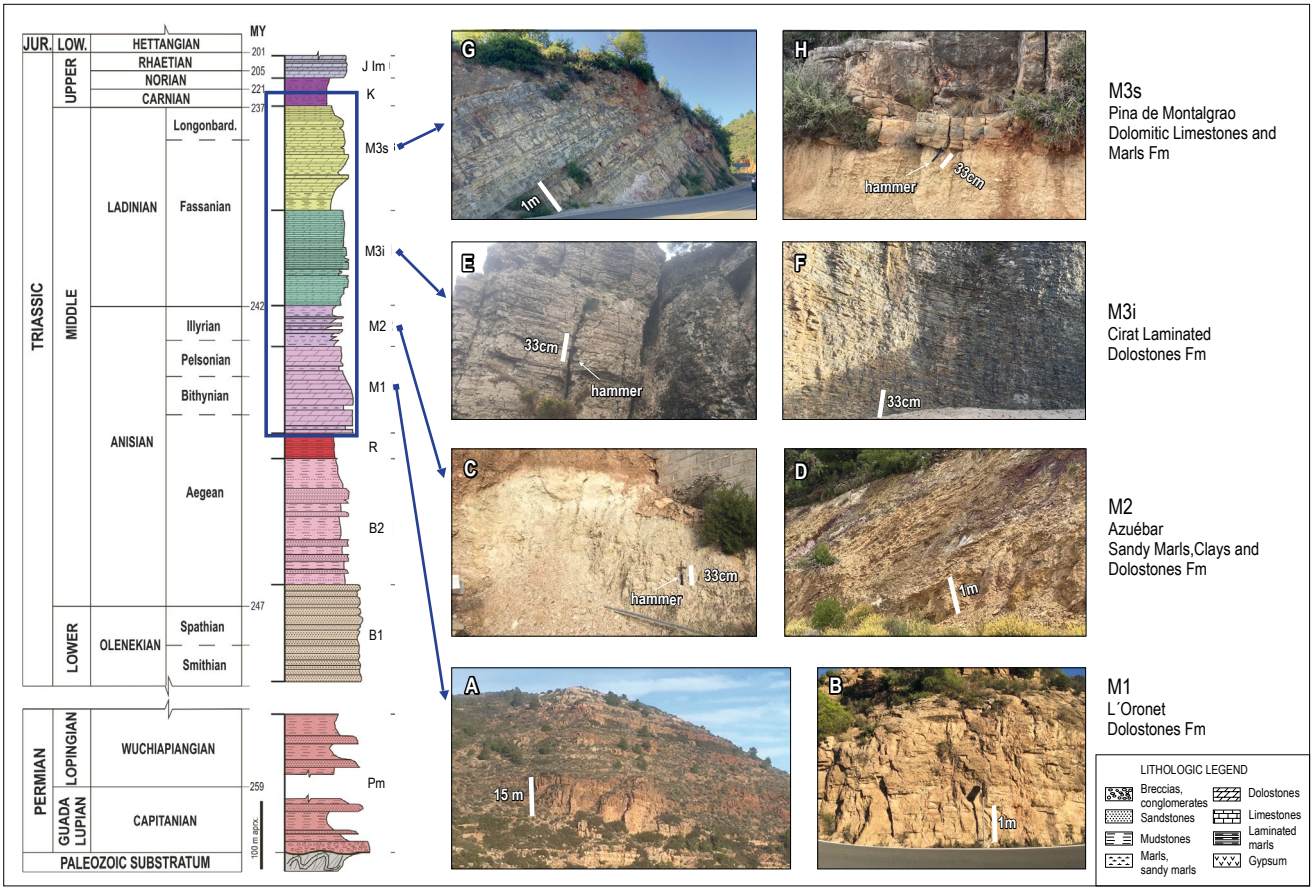

FIGURE 5. Synthetic lithostratigraphic section of the Permian-Triassic formations and units in the Sierra del Espadán and Sierra Calderona domains (adapted from Hernaiz-Huerta, 2023, 2024a) and pictures of characteristic outcrops of the Muschelkalk formations described in the text. Initials of geological units, as in Figure 3. J Im: Imón Fm.

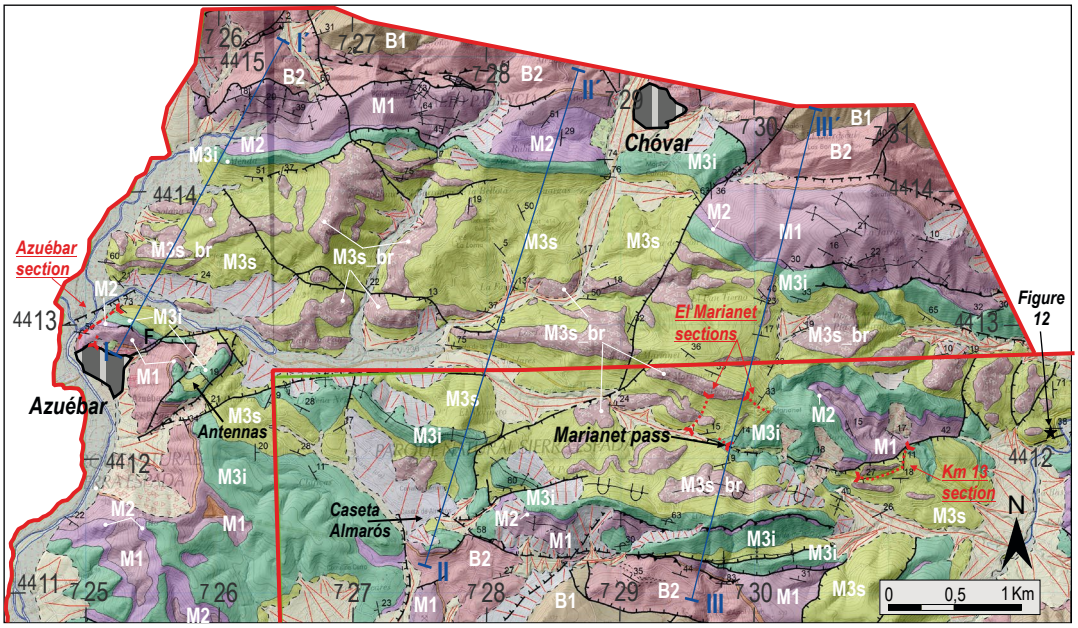

FIGURE 6. Detail of the NW sector of the geological map in Figure 3 (upper left inset). Legend as in Figure 3. I-I' to III-III' refer to the traces of the geological cross-sections shown in Figure 16. The location of Azuébar, Km-13 and Marianet sections is indicated in red colour. The letter F in black colour close to Azuébar village shows the location of the fault depicted in Figures 7A and 8B. The outcrop shown in Figure 12 is marked with a black star.

40m, but it may disappear locally by extreme thinning and wedging. This formation is made of clays, siltstones and sandy marls with typically yellowish colours, sometimes whitish due to alteration and occasional reddish hues, which intercalate centimetre-scale layers of marly sandstones, dolomitic limestones, and dolostones of the same coloration (Fig. 5C, D). Garay (2001) referred to these lithofacies as "Almedijar type", due to their resemblance to those previously described in the Almedijar locality of the Sierra del Espadán, relatively close to the study area (Hernández *et al.*, 1985a, b). Other outcrops of this unit, however, show lithofacies closer to the 'Chelva type' (Hernández *et al.*, 1985a) with dominant reddish clays and marls that locally may include gypsum layers. This 'Chelva type' lithofacies characterize the M2 in the Triassic realms that surround this village about 40-50km to the west of the study area.

Above the previous unit, Garay (2001) distinguished two formations, which he named the Cirat Fm and the Pina de Montalgrao Fm, in stratigraphic order. He equated the first with the characteristic M3 of thin (5-15cm), well bedded dolostones and recognized the second as equivalent to the "Royuela Beds" of the western sectors of the Iberian Range (Pérez-Arlucea and Sopeña, 1985), proposing for it a new designation as M4 within the Muschelkalk. In the new mapping, these two units are included in the M3, assigning the first to a lower M3 (M3i) and the second to an upper M3 (M3s).

The Cirat Fm (M3i), consists of a relatively monotonous succession of cm-scale well bedded, slightly undulating dolostones with dark grey tones, often laminated, with occasional interbeds of marly layers (Fig. 5E, F). Its thickness in the mapped area varies between 50 and 80 meters. The Pina de Montalgrao Fm (M3s) thoroughly outcrops conformable and transitional above the former, with very characteristic facies composed of an alternation of pinkish thin bedded and laminated marly dolostones and limestones, yellowish, sometimes reddish, fined grained clayey sandstones, and whitish laminated marls (Fig. 5G). Upwards in the section, these marls become predominant and usually include intercalations of the other mentioned lithologies (Fig. 5H). According to Garay (2001), this unit transitions directly into the Keuper, as described in its type section.

Pérez-López *et al.* (2021) conducted a detailed sedimentological study of the carbonate units of the Muschelkalk (M1 and M3) in two different areas of the NW sector of the Sierra del Espadán (Alt Palancia and Sierra Manzanera). Through a comprehensive analysis of their facies associations, these authors concluded that both units arrange as similar transgressive-regressive cycles belonging to a very shallow epicontinental platform environment, each one represented by massive carbonate facies bounded by mixed or lagoon-type tidal flats deposits, the M3 facies being slightly deeper. The poor quality of the M2 outcrops restricts any interpretation of its sedimentary environment. However, based on its stratigraphic position and dominant lithologies, M2 is interpreted as the culmination of the regressive cycle that concludes the underlying M1 carbonate unit (L´Oronet Fm) and the transition to the subsequent marine transgression marked by the onset of the M3i carbonate unit (Cirat Fm). The extent to which sabkha-type evaporitic environments prevailed during this interval would have influenced the local predominance of "Chelva-type" facies over "Almedijar-type" facies.

The paleontological content is very sparse in M1, and slightly more abundant in M3. It mainly consists of bivalves and gastropods, along with secondary brachiopods and echinoderms, and occasional isolated ammonites (*e.g.* Escudero-Mozo *et al.* 2015; López-Gómez and Arche, 1992). This fossil content does not always warrant a precise dating. Palynological data obtained by Ortí *et al.* (2020) in the Alt Palancia area of the Sierra del Espadán consistently assign an Anisian age to M1, identifying associations corresponding to the Aegean/Bithynian in the lowermost part of the unit and to the Bithynian-Pelsonian in the upper part. These authors constrain the age of M2 to the middle to upper Anisian (mainly Illyrian). All samples collected from M3 indicate a Fassanian age (lower Ladinian), without entirely clear specimens or associations representative of the Longobardian (upper Ladinian) (Ortí *et al.*, 2020). The youngest age of M3 is thus constrained to the boundary with the Carnian, or possibly even below it. These palynological ages (Figs. 3; 4; 5) are generally slightly older than those obtained for the same units using the same method by other authors in the central and western sectors of the Iberian Range (Doubinger *et al.*, 1990; López-Gómez and Arche, 1992). In a recently published review of the Middle Muschelkalk of the Valencian sector of the Iberian Range, Ortí *et al.* (2025) have reported a palynological assemblage found in "Chelva-type" facies of the M2 near this locality, which they assign close to the Anisian–Ladinian boundary, and another from the base of the Keuper (K1), which they date as early Carnian.

RESULTS

The M2 record in the study area

In the study area, the M2 usually crops out as a thin low-competent level in "Almedijar type" facies, separating the carbonate M1 and M3 units. Some of its outcrops partially exhibit the appearance of "Chelva type" facies, but contrary to what occurs in Sierra Calderona (Garay, 2001; Hernaiz-Huerta, 2022, 2024a), no gypsum has been found in any of them.

The omission of this unit due to rapid thinning can be observed on the hills surrounding the locality of Azuébar. Both in the hill where the Azuébar castle settles and in the escarpments situated to the south, east and southeast, the progressive wedging out of this unit can be followed in the field and mapped (Figs. 6; 7A; 8B). Figure 8A shows a lithostratigraphic section logged from the contact with the underlying Röt facies, close to the village's water deposit (Fig. 7A) up to the M3i (Cirat Fm)-M3s (Pina de Montalgrao Fm) contact. The observations have been complemented with the exposures along the road leading out of the village towards Alfondeguilla (Fig. 8B). This section records nearly 100m of M1 (L'Oronet Fm), a maximum of 35-40m (in the road transect, mostly covered) of M2 (Azuébar Fm) and 45-55m of M3i (Cirat Fm). Above the Cirat Fm, some few meters of M3s (Pina de Montalgrao Fm) outcrop below a set of massive breccias that can be assigned to the "supra-Pina de Montalgrao Fm" (see below). In plan view (Fig. 6; 7A; 8B) the M2 unit shows a progressive thinning towards the eastern end of this hill, probably accentuated by local thrusting of the M1 unit above it at the castle transect. Similarly, in the hills south of Azuébar, the mapping reveals a rapid northwards thinning of M2, which completely wedges out approximately 1km south of the Antennas site (Fig. 6). An evident thinning trend is also observed in the underlying M1 unit.

In the Azuébar section (Fig. 8A), the M1-L'Oronet Fm is composed of metric-scale, medium to thick-bedded, dominantly fine-grained, thickening-upwards dolostone (and minor limestone) cycles. The main sedimentary structures consist of bioturbation affecting the marly intervals, bird-eye structures, fossil molds and localised cross-bedding. In the lower part of the succession, there is a prominent continuous 10-12m thick, light-coloured interval of stromatolites (interval 2 in Fig. 8A, B) showing stratiform and domal structures. Stromatolites are also dominant in the uppermost part of the unit, where they

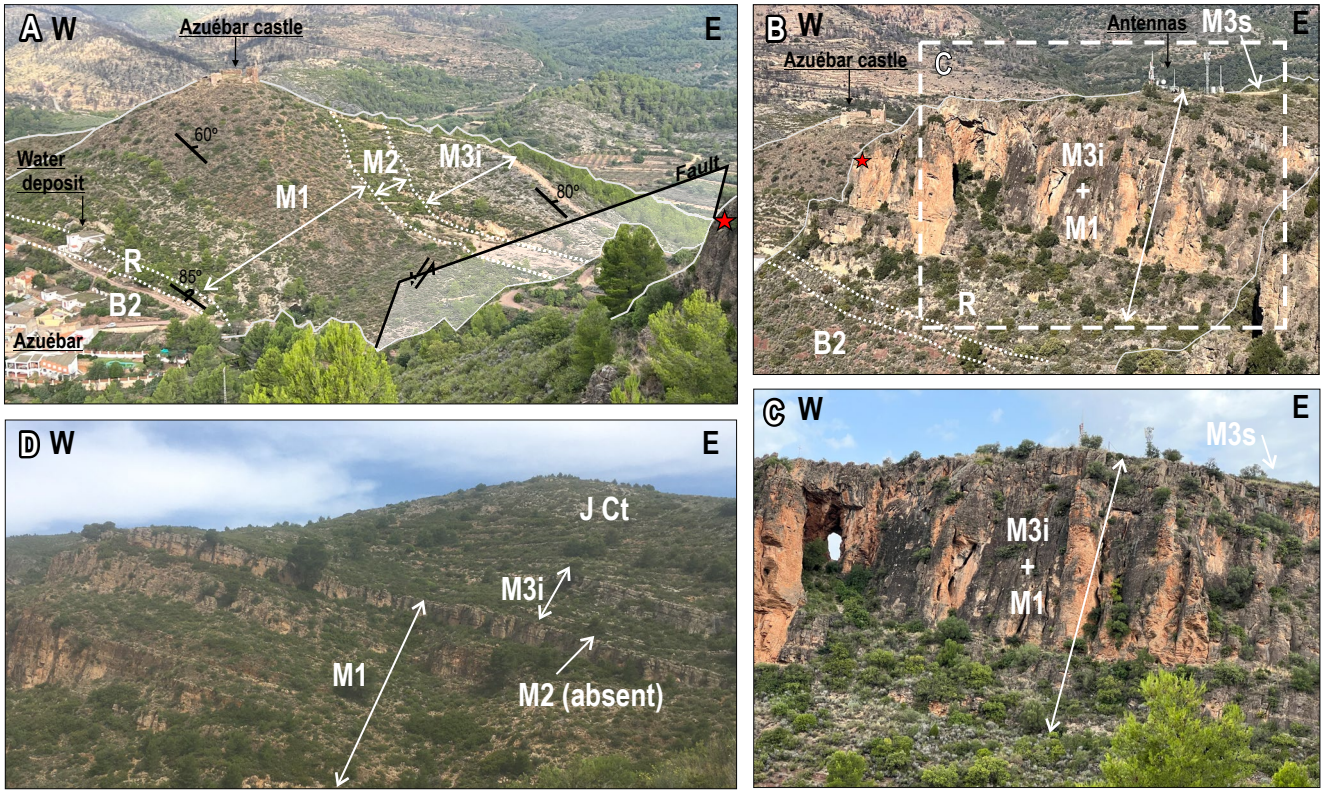

FIGURE 7. Field view of Muschelkalk M2 unit wedging and omission in the Azuébar area (see text for explanation). A) Westwards view of the continuous Triassic succession comprising from uppermost Buntsanstein B2 up to M3i units bearing a steep dip (50-80º) towards the NNE, locally sub-vertical or slightly inverted, immediately north of the locality of Azuébar. The scarce thickness (10-15m) of the less competent M2 unit between the dolomitic outcrops of M1 and M3i is noted. The fault that bounds the Azuébar block to the East is labelled as F on the map in Figure 6. The red star marks the position of the dolomitic escarpment depicted in B. B, C) Panoramic views of the dolomitic escarpment located to the E/SE of A. The escarpment consists of a continuous succession of M1+M3i dolostones, approximately 100 meters thick, with complete omission of the M2. At the base of this succession, a thin (≈20m) package of red and green/grey laminated siltstones, claystones and marls with thin intercalations of yellowish carbonates belonging to the Röt facies (R) culminate the red mudstones and sandstones of the Buntsandstein B2 unit. The alternation of the laminated marls, marly dolostones and limestones of the Pina de Montalgrao Fm overlies the dolomitic succession at the level of the Antennas. D) Continuous dolomitic succession of M1+M3i, with total absence of M2 in the Les Coves area of the Sierra Calderona, as cited in the text. The initials (in solid white color) refer to the geological units or formations, as in the legend of Figure 3.

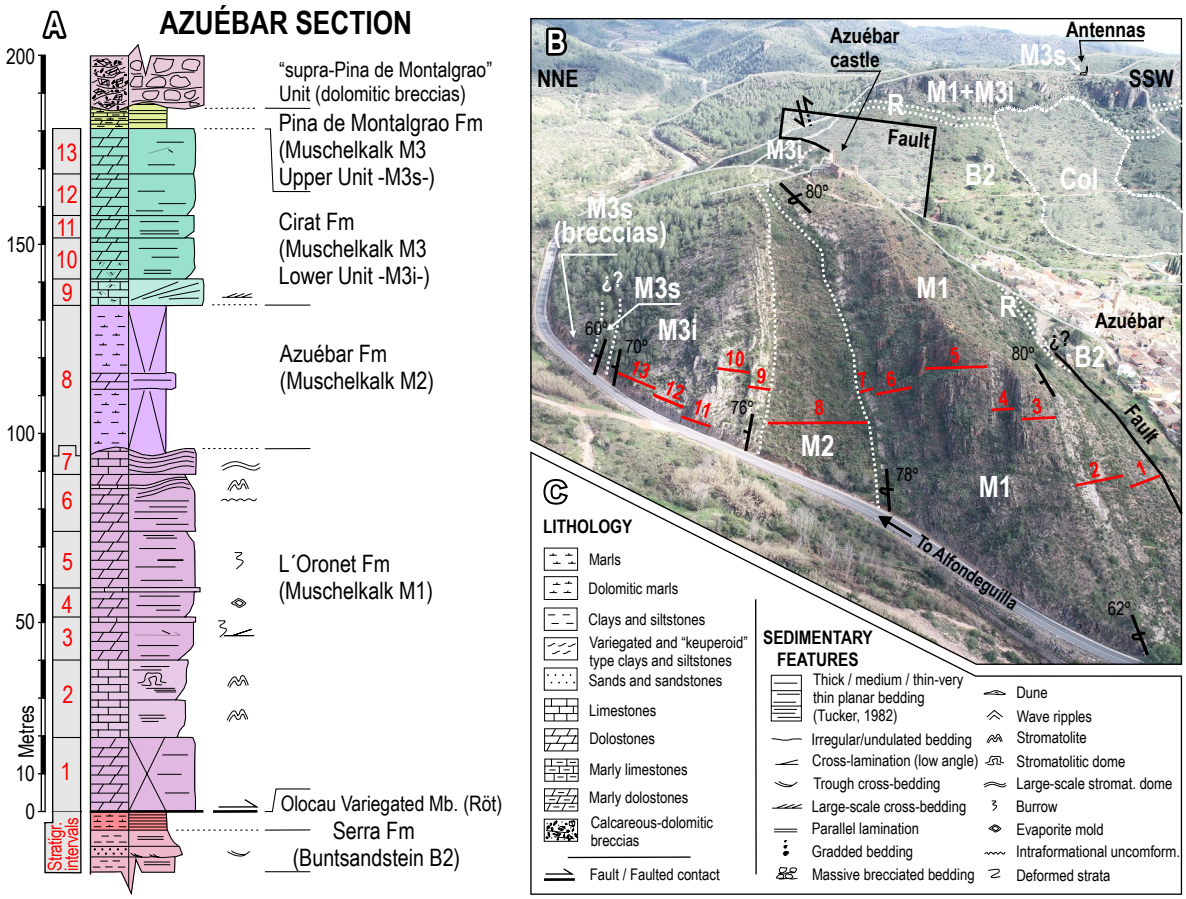

FIGURE 8. The Azuébar section (see text for explanation). A) Lithostratigraphic section of the Muschelkalk (M1+M2+M3) succession north of the village of Azuébar. B) Foreground: dron view (looking eastwards) of the Azuébar section depicted in A along the Alfondeguilla roadcut. The stratigraphic intervals (1 to 13) considered in the section are indicated in red colour. Note the location of Azuébar castle for comparison to Figure 7A. Background: the location of the escarpments and antennas site mentioned in Figures 7B and C, is shown. The fault is the same depicted in Figure 7A, labelled with a black F letter in the map of Figure 6C) Common legend for lithology and sedimentary features applying to all the lithostratigraphic sections included in this work.

form large-scale mounds (intervals 6 and 7 in Fig. 8). Above the incompetent, altered and mostly covered M2 unit, the M3i-Cirat Fm exhibits lithologies comparable to those of the M1, with thinner beds and cycles. The basal interval consists of well-stratified thick beds of carbonate breccias, showing large scale cross bedding with downlap geometry. Towards the middle-upper part of the section, small-scale cross lamination is present. The facies in M1 and M3i are consistent with the shallow carbonate platform setting assigned to these two units by previous authors (*e.g.* Garay, 2001; Perez-Lopez *et al.*, 2021).

In contrast, the escarpment east of the village, on which the antennas are placed, is entirely formed by a continuous succession of well-bedded dolostones (Fig. 7B, C). This M1+M3i succession (overall also thinned to around 100m) overlies the Röt facies (R) which culminates the Buntsandstein B2 unit and is overlain by the Pina de Montalgrao Fm (M3s).

An equivalent situation can be observed on the hill south of Caseta de Almarós (Figs. 3; 6) where a M1+M3i continuous succession is extremely thinned to 40-50m. The same pattern can be recognised in the dolomitic succession hosting the renowned San Josep caves of La Vall d'Uixó, along the road section from this locality towards Alfondeguilla (Fig. 3), where the M2 is reduced to less than 1m.

Despite its lesser representation compared to the La Vall d'Uixó sector of the Sierra del Espadán, the thinning and eventual local omission of the M2 has also been described and mapped at specific locations in the Sierra Calderona (Fig. 7D) (Hernaiz-Huerta, 2022), confirming this trend at a regional scale.

The M3 in the study area: the "supra-Pina de Montalgrao" facies

The Cirat Fm (M3i) and the Pina de Montalgrao Fm (M3s) show distinct facies throughout the mapped area in

the upper part of the Muschelkalk succession. However, the facies described for the Pina de Montalgrao Fm do not culminate this succession in the study area. Instead, they are followed by massive, predominantly marly-clayey facies, often variegated and "keuperoid" in type, which intercalate frequent layers and packages of thin well bedded and laminated dolostones, similar to those in the M3i unit, and abundant packages of carbonate breccias, sometimes with carniolar appearence. These breccias are the most defining feature of this uppermost part of the Muschelkalk in this area. Although, in general, the "keuperoid" marly-clayey facies does not include intercalations of gypsum beds, these have been identified in some isolated locations, two of them close to the Azuébar village (X/Y-UTM coordinates: 724494/4413439 and 725260/4413316) and the other close to Km-point 15 of the Azuébar-Alfondeguilla road (732360/4412365). Other outcrops of this facies show disperse small crystals of gypsum.

The contact between these massive marly-clayey "keuperoid" facies and the underlying well stratified facies of the Pina de Montalgrao Fm has not been mapped, as it is very gradual and difficult to demarcate due to the incompetent nature of both deposits. In addition, intervals of facies typical of Pina de Montalgrao Fm can be often found at different stratigraphic levels within the massive "keuperiod" marls and clays, reflecting lateral facies changes between them. For these reasons, these new facies have been provisionally retained within the M3s unit, *i.e.* not differenciated from it (Fig. 9), although both the breccias and the dolomitic intervals, when forming bodies of notable thickness and showing sufficient mapping entity, have certainly been distinguished in the map (M3s_br unit in the map and legend of Figs. 3; 6). Provisionally and informally, these are here referred to as the "supra-Pina de Montalgrao" facies or unit (or, simplified, "supra-Pina" facies or unit) (Fig. 9). A more precise definition and stratigraphic assignment of these facies, however, will require further dating.

These "supra-Pina" facies outcrop throughout the mapped area (Fig. 3) but are especially abundant along an east-west trending synclinal or synclinorial strip of kilometre-scale width that runs approximately between Alfondeguilla, Azuébar and Chóvar in the NW part of it (mostly included in Fig. 6), which behaved as a small, localized basin (see below). Good exposures of the unit are accessible along the road between the two former localities and a parallel track at a lower elevation. A key mapping site is the Marianet Pass (Coll de Marianet; Figs. 3; 6; 10A), where the contact between the thin, well-bedded dolostones of the Cirat Fm (M3i; Fig. 10B) and the

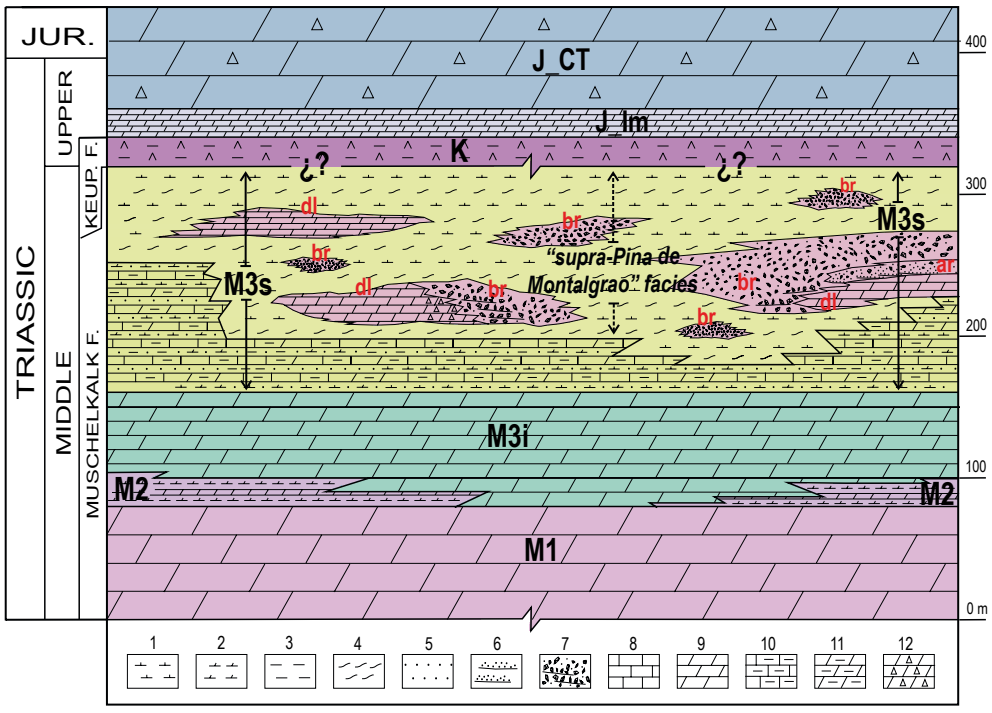

FIGURE 9. Idealized stratigraphic diagram of the Muschelkalk in the study area. The thicknesses (scale on the right) are approximate. Unit abbreviations as in Figure 3. J_Im: Imón Fm; J_CT: Cortes de Tajuña Fm. The abbreviations in red indicate the predominant lithologies within the M3s_br unit: dl= dolostones; br= breccias; ar= quartz-rich sandstones and microconglomerates. Lithologies: 1. marls; 2. dolomitic marls; 3. clays and siltstones; 4. variegated and "keuperoid"-type clays and marls; 5. sands and sandstones; 6. channeled sandstones and microconglomerates; 7. calcareous-dolomitic breccias; 8. limestones; 9. dolostones; 10. marly limestones; 11. marly dolostones; 12. carniolar limestones and dolostones.

stratified marly-calcareous and dolomitic succession of the Pina de Montalgrao Fm (M3s; Fig. 10C) is clearly exposed. Westwards, towards Azuébar, this succession transitions into massive, variegated marly-clayey "keuperoid" facies (Fig. 10D). These facies, along with thick (>10–20m) packages of well-bedded dolostones and breccias (M3s_br), are extensively exposed along the road and on the hillside tracks (Fig. 10E, F, G)

Two lithostratigraphic sections were logged on the slope north of the Marianet Pass to assess the relationship between the Pina de Montalgrao Fm and the overlying "supra-Pina de Montalgrao" facies (Fig. 11). The eastern Marianet (E-Marianet) section primarily comprises alternating marly dolostones and limestones, with interbedded marls of the Pina de Montalgrao Fm and a ~5m thick interval of "keuperoid" facies in its lower part. The uppermost unit is a >10m thick, fine, well-bedded dolostone (M3i-type), which thickens westwards into the top of the western Marianet (W-Marianet) section. In the W-Marianet, this dolostone overlies "keuperoid" facies well-exposed in the road cut, situated above the Pina de Montalgrao Fm A second, 15–20m thick dolostone package occurs mid-section, interbedded within this "keuperoid" facies, showing good westwards continuity but abruptly wedging eastwards. Overall, the Marianet sections reveal the vertical and lateral transition of the Pina de Montalgrao Fm into the "supra-Pina de Montalgrao" facies (dolostones intervals

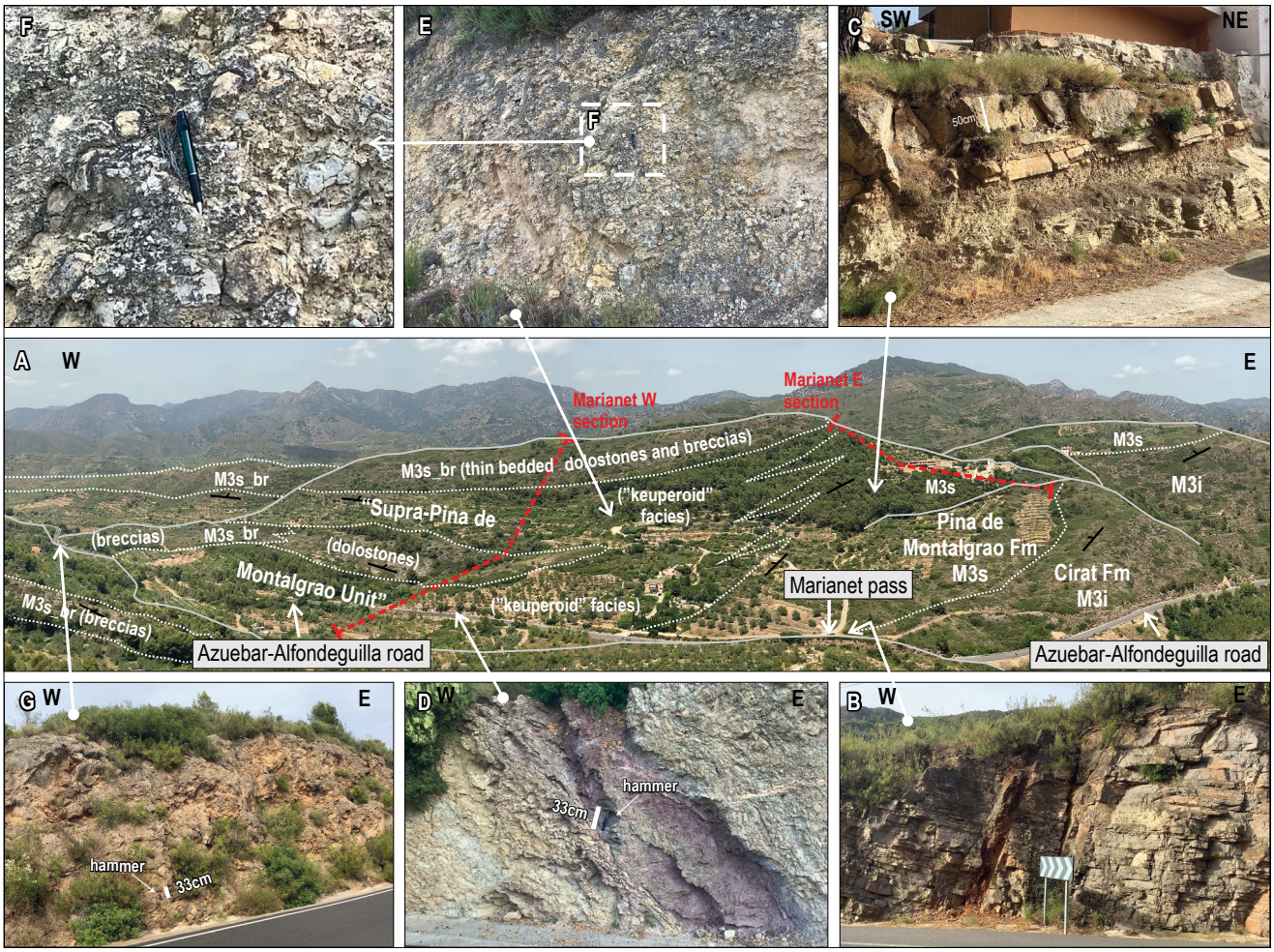

FIGURE 10. Spatial distribution and field view of the Muschelkalk M3 units in the Marianet Pass area. A) Panoramic view (facing North) of the M3 units occurrence in the Marianet Pass (see maps in Figures 3 and 6, respectively, and the explanation in the text). Location of El Marianet-E and W lithostratigraphic sections shown in Figure 11 is indicated. B) Uppermost part, near the top, of the thin bedded and laminated dolostone succession of the Cirat Fm (M3i) in the Marianet Pass. C) Alternation of laminated marls and marly dolostones and limestones of the Pina de Montalgrao Fm on the track leading up to the El Marianet farmhouse. D) Variegated "keuperoid" clays and marls overlying the Pina de Montalgrao Fm to the West of Marianet pass This lithology forms the main body of the "supra-Pina de Montalgrao" facies in this sector. E, F) Interval of calcareous-dolomitic breccias (M3s_br) intercalated in the "supra-Pina de Montalgrao" "keuperoid" facies, outcropping in a roadcut of the track leading up to the El Marianet farmhouse stratigraphically above and in lateral transition with the unit shown in inset C, G) Massive calcareous-dolomitic breccias, partially with a carniolar appearance (M3s_br), included in the "supra-Pina de Montalgrao" facies, intersected by the Azuébar-Alfondeguilla roadcut (PK 10+600 approximately).

included), which, in some cases, may even overlie the former unconformably (Fig. 11).

At the mapping scale, it is sometimes possible to trace the transformation of "M3i-type" dolostones embedded within the marly-clayey "keuperoid" matrix into breccias. A clear example of this process is the second dolostone unit in the W-Marianet section, which reappears in a roadcut approximately 700m further west, where it is entirely transformed into a massive breccia unit, as illustrated in Figure 10G. The in-situ disaggregation and fragmentation of the "M3i-type" dolomitic packages into breccias can be observed in detail in other outcrops (see Fig. 12).

The "keuperoid" facies occur both with and without interbedded dolomitic and carniolar beds, but consistently lack gypsum with the exceptions mentioned before. Beginning at approximately Km-point 13 of the Azuebar-Alfondeguilla road and conformably overlying the Cirat Fm (M3i) (Fig. 13A), a lithostratigraphic section was logged (westwards), revealing a wide array of subfacies typically associated with this "keuperoid" main lithology, such as (Fig. 13): i) thin-medium-bedded layers to thick packages of dolomitic breccias composed of centimetre-sized fragments of dark-grey dolostones embedded in a millimetre-sized matrix of similar composition or intermixed with the marly-clayey host material (Fig. 13B); ii) thin to medium-bedded intervals of finely laminated clays and dolomitic marls (Fig. 13C); iii) more competent medium- to thick-bedded units developed where dolomitic marl intervals thicken and become richer in dolomite, giving rise to thin-bedded marly dolostones with subordinate limestones (Fig. 13H).

In the middle and especially in the upper part of the section, the "keuperoid" facies become increasingly enriched with fine- to medium-bedded, coarse-grained

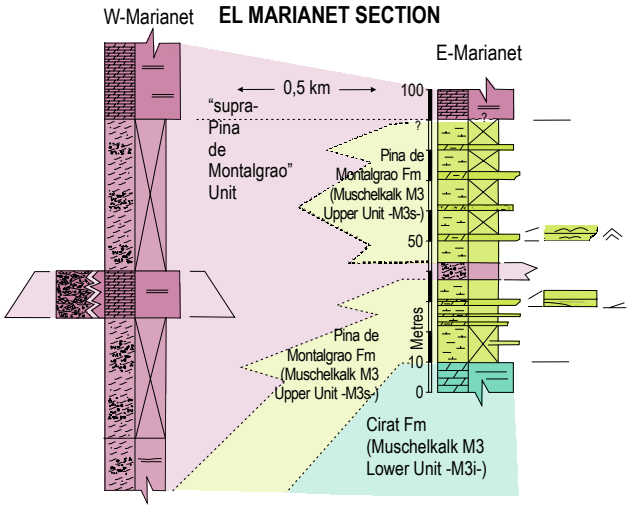

FIGURE 11. Correlation of E-Marianet and W-Marianet lithostratigraphic sections. See text for explanation- Symbology as in Figure 8B. The location of both sections is shown in Figure 10.

quartz-rich sandstones and granule or pebble conglomerates (Fig. 13F, G) frequently exhibiting low-angle cross-bedding (Fig. 13E) and, in some cases, forming channelized bodies (Fig. 13I). These siliciclastic intervals tend to thicken and coarsen upwards, concurrently with the thickening of dolomitic marl and marly dolostone layers. They may alternate with laminated red claystones and together form decimetre to meter-thick thinning upwards superimposed cycles.

Throughout the entire section the "keuperoid" facies show evidence of internal deformation such as irregular or undulating bedding, frequent disruption of stratification, abrupt intra-formational unconformities (Fig. 13D), and local, discontinuous decametric-scale folding (Fig.

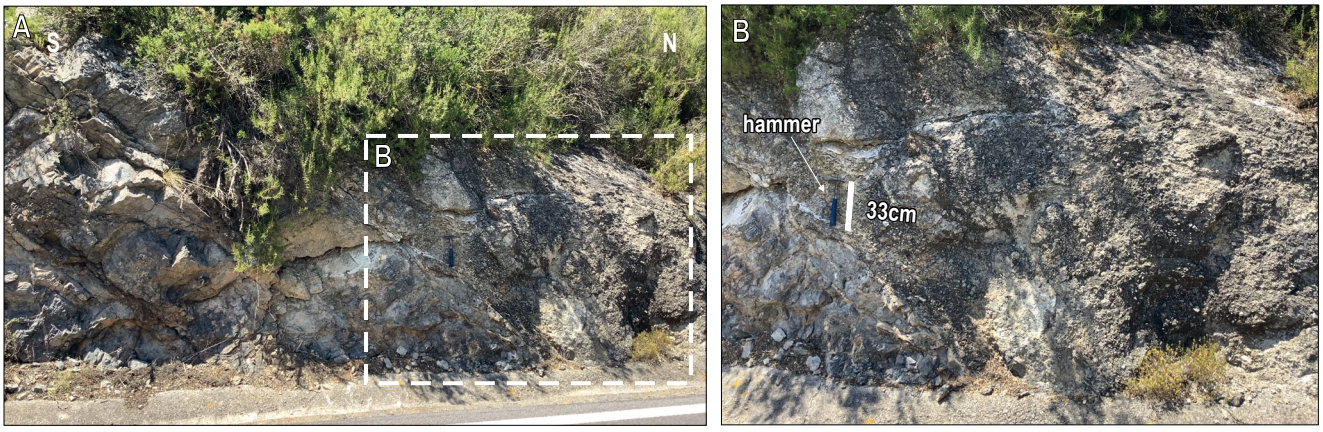

FIGURE 12. Example of the brecciation process. A) Outcrop of thin to medium well-bedded and laminated dolostones of "M3i type" embedded in the "keuperoid" facies of the "supra-Pina de Montalgrao unit that laterally and upward transition to calcareous-dolomitic breccias. B) Detail of the breccias horizon. PK 14+900 of the Azuébar-Alfondeguilla road (east of the Marianet Pass; see location in the map of Figure 6). See hammer for scale (33cm).

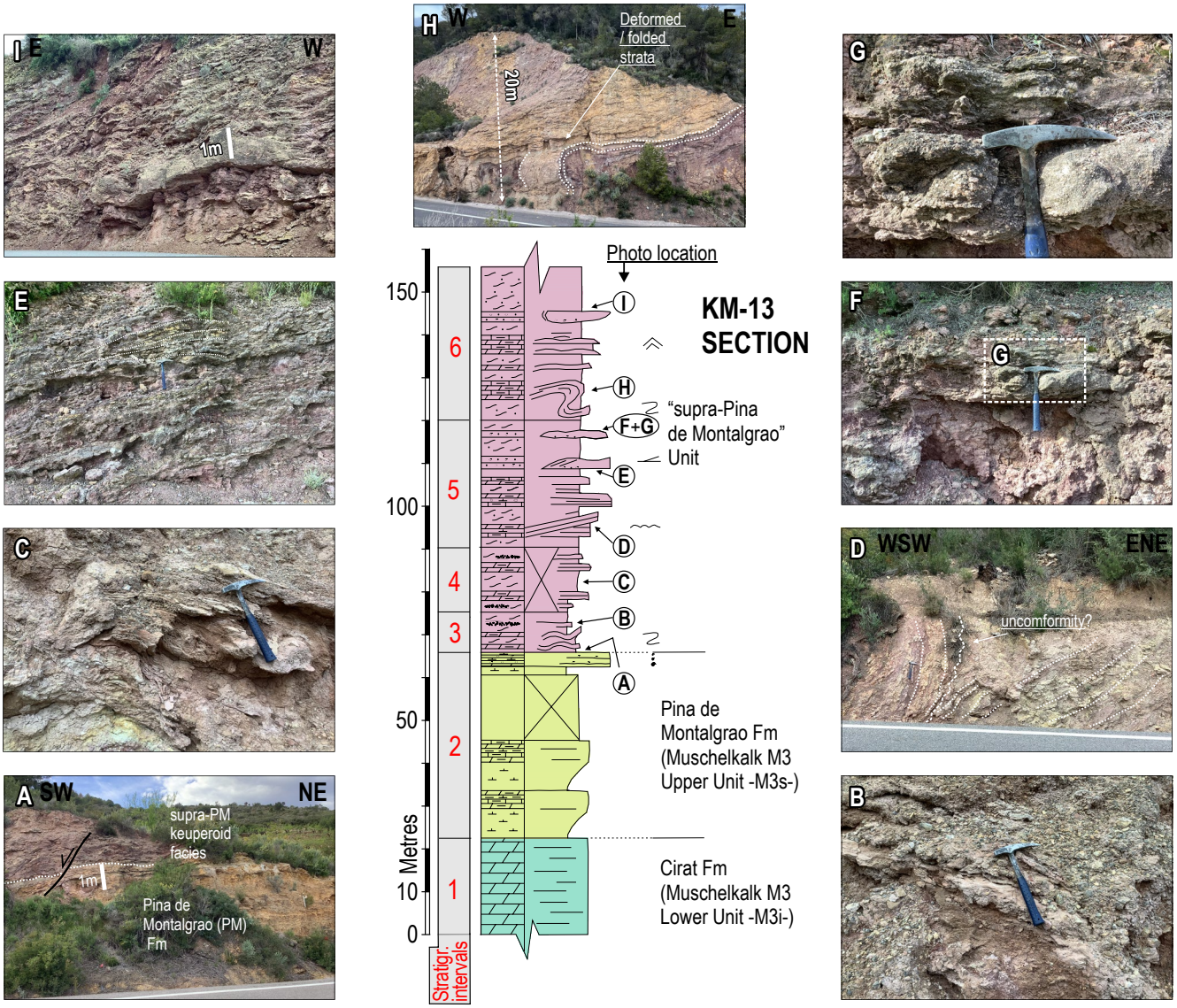

FIGURE 13. Azuébar-Alfondeguilla road Km-13 lithostratigraphic section and examples of related lithologies. Location of the pictures in the section are indicated with the corresponding labels. See text for explanation. A) Good exposure of the Pina de Montalgrao Fm-"supra-Pina de Montalgrao" "keuperoid" facies contact. B) Package of dolomitic breccias intercalated in the "keuperoid" facies. The breccias are embedded in a millimetre-sized matrix of similar dolomitc composition or intermixed with the marly-clayey host material. C) Horizons of finely laminated clays and dolomitic marls interbedded with the "keuperoid" facies. D) Internal (intra-formational?) unconformity between two sets of layers forming the keuperoid facies; E) Thinning-upward, superimposed cycles of siliciclastic sandstones and granule-to-pebble conglomerates overlain by laminated red claystones, representing the main lithology of the "keuperoid" facies in this part of the section. Note the broad, low-angle cross-bedding in the layer immediately above the hammer. F, G) Details of fine- to medium-bedded layers of coarse-grained quartz-rich sandstones and granule or pebble conglomerates comprised in the "keuperoid" facies. H) Decametre-scale internally deformed/folded layers of competent medium to thick-bedded marly dolostones and limestones. I) Channelized, laterally discontinuous body of siliciclastic sandstones and microconglomerates intercalated within the "keuperoid" facies.

13H). The "keuperoid" facies as a whole are difficult to interpret, and it is posibble that their common lack of sedimentary structures, or even some features that appear to be such, are in fact the result of tectonic or diagenetic processes (see below the Discussion section). Additional specific studies, beyond the scope and objectives of the present work, will be required to evaluate the different possibilities.

The massive marly-clayey "supra-Pina de Montalgrao" facies are extensively distributed across the rest of the mapped area. Additional significant outcrops include the slopes near the L'Alfinac petrol station, situated east of the A7 highway at kilometer point 289, as well as several exposures in the vicinity of the town of La Vall d'Uixó (Fig. 3). Particularly noteworthy is the abandoned La Pedrera quarry, situated near the northeastern margin of the

town's urban area, which offers exceptionally well-exposed sections of these facies (Fig. 14). Consistently with observations made at other points within the mapped area, the contact of the "supra-Pina de Montalgrao" facies with the underlying Buntsandstein B2 unit in the Pedrera quarry area has been interpreted as a low-angle normal fault with the fault plane becoming steeper towards the west.

Figure 15 shows a composite lithostratigraphic section based on observations from the northern and southern fronts of the La Pedrera quarry. At the northern front (Fig. 15A), a basal interval of reddish "keuperoid" clays and marls (Fig. 15C) is overlain by ~10m of coarse quartz-rich sandstones and microconglomerates (Fig. 15D, E), with interval 3 distinguished by darker tones and prominent cross-stratification (Fig. 15E). These siliciclastic deposits, comparable to those at Km 13 (Fig. 13), remain continuous and dominant throughout this entire set. Above them, "keuperoid" facies reappear, now containing dispersed breccias within a marly-clayey matrix (intervals 5 and 6; Fig. 15A, B), observed in both quarry fronts.

At the southern front (Fig. 14, point 2), overlying partially sandy marly-clayey strata (intervals 7 and 8), a 10–15m thick dolomitic megabreccia is well exposed (Fig. 15B). It consists of meter-scale fragments of well-bedded, dark-grey dolostones (Fig. 15F) embedded within coarse sand to microconglomerate-sized matrix (Fig. 15G, H), and shows large-scale cross-bedding despite its massive appearance. The breccia thickens westwards, exceeding 30m in the westernmost quarry sector (Fig. 14)

The set of facies and subfacies described in this section suggests an evolutionary transition from partially restricted epicontinental shallow water marine environments, characteristic of the Muschelkalk M3 as a whole, to markedly restricted settings such as sabkha or lagoon-type environments, which primarily governed the deposition of the "keuperoid" facies that define the "supra-Pina de Montalgrao" unit. Within these restricted environments, the siliciclastic facies together with their interbedded laminated claystones represent external inputs deposited in ephemeral fluvial or fluvio-tidal systems. Nevertheless, these predominantly restricted settings alternated with episodes of renewed shallow marine conditions, as evidenced by the frequent intercalations of tabular and laminated dolomites of the M3i type. This entire depositional evolution likely occurred within a context of tectonic instability, which could account for the abundance of breccias, possible intra-formational unconformities, and syn-depositional deformation of strata.

The thickness of the "supra-Pina de Montalgrao" facies and the upper part of the Pina de Montalgrao Fm itself are difficult to estimate due to their inherently incompetent

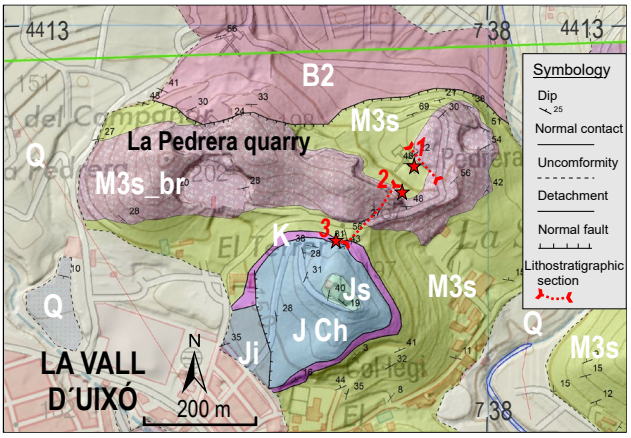

FIGURE 14. Geological map of La Pedrera Quarry area, enlarged from Figure 3. Legend as in Figure 3, except for: Ji= undiferenciated Lower Jurassic; JCh= Chelva Group (Middle Jurassic); Js= undiferenciated Upper Jurassic. Points 1 and 2 indicate the location of the northern and southern quarry fronts, respectively, as referred in the text and in Figure 15. The approximate trace of the composite lithostratigraphic section depicted in Figure 15 is indicated. Point 3 shows de location of pictures shown in Figure 17. Green line marks the boundary of the 1:25,000 scale Vall d'Uixó sheet.

nature. The thickest successions occur in the NW sector of the study area, between the Marianet Pass and Azuébar and Chóvar villages, where they include abundant and thick intercalations of thin well-bedded dolostones and breccia packages (Fig. 6). Cross-sections drawn in this sector (Fig. 16) with the aid of a large number of dip data (Fig. 6) suggest the development of a basin roughly coincident with the synclinal structure. In this basin, the "supra-Pina de Montalgrao" facies, with an undetermined top, exceed 150-200m in thickness, and in certain points along its central (section II-II') and eastern (section III-III') transects, may reach over 300m. The underlying Pina de Montalgrao Fm, with an average thickness of 100-150m, also increases significantly in thickness along the central transect of the basin, where it can exceed 400m near the northern margin due to a facies transition to the overlying unit. In summary, in the NW sector of the study area, the entire upper M3 succession (M3s) can reach a minimum (visible) thickness of approximately 500m. Of these, the "supra-Pina de Montalgrao" facies account for 150 to 350m depending on the transect, and the underlying Pina de Montalgrao Fm accounts for average 100-150m, with a substantial increase up to 400m along the central transect (II-II´ in Fig. 16).

DISCUSSION

Implications of the occurrence of Muschelkalk M1 and M2 in the study area

The new 1:25,000 scale mapping of the SE sector of the Sierra del Espadán near La Vall d'Uixó proves the continuous

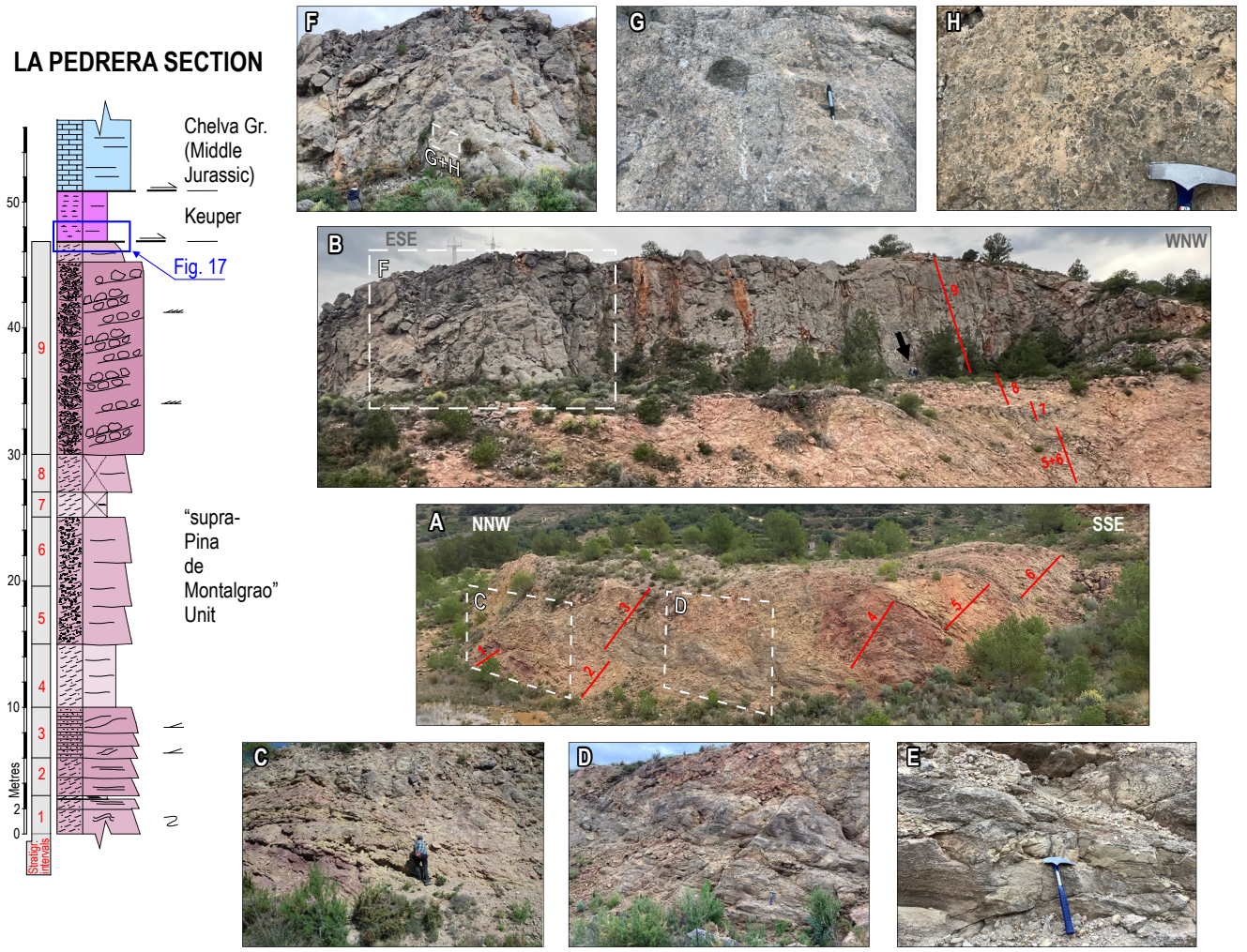

FIGURE 15. La Pedrera (quarry) lithostratigraphic section and examples of related lithologies. See location in Figure 14. The stratigraphic intervals (1 to 9) considered in the section are indicated in red colour. The blue box shows the stratigraphic position of Figure 17 in the section. See text for explanation. A) Northern quarry front. B) Southern quarry front. The black arrow shows the location of two people for scale. C) Typical appearance of the "supra-Pina de Montalgrao" "keuperoid" facies at the bottom of the section (interval 1). D, E) Succession of quartzitic sandstones and microconglomerates represented as 2+3 intervals in the section, showing a well-developed low-angle cross-stratification. F) Superb outcrop of the massive mega-breccia exposed in the southern quarry front (interval 9). The blocks within the mega-breccia have an average size of 20-40cm and can reach up to 1m in diameter. These blocks are composed of angular to slightly rounded fragments of dark-grey, thin-bedded M3i-type laminated dolostones and are embedded in a coarse sand/microconglomerate-sized matrix of the same composition. G, H) Details of the mega-breccia at the bottom of the quarry front (interval 9).

occurrence of the M2 marly-clayey unit, preferentially in "Almedijar type" facies, throughout the surveyed area, even in the outcrops closest to the coast. This confirms previous reports in different areas of the region (Elorza and Pedraza, 1973; Garay, 2001; Hernaiz-Huerta, 2022, 2024a; Ortí *et al.*, 2020, 2025) although ideally, further datings could serve to substantiate this interpretation. Garay (2001) identified and mapped the M2 unit throughout both Sierra del Espadán and Sierra Calderona and described about 10 key lithostratigraphic sections within them. The thickness of the M2 is generally quite reduced (10-30m), and the unit can even locally disappear, not necessarily near the coast, due to wedging or facies changes. In such case there is a continuous carbonate succession formed by the M1+M3i units. According to these observations, it is necessary to re-examine the inclusion of Sierra del Espadán and the Sierra Calderona within the Levantine-Balearic Triassic domain (Escudero-Mozo *et al.*, 2015; López Gómez *et al.*, 1998).

Special mention deserves the proposal by Escudero-Mozo *et al.* (2015) to assign the entire Muschelkalk dolomitic succession in the eastern sector of the Iberian Range to the M3. Lopez-Gomez and Arche (1992) had previously identified the extensive outcrop of the M1 (lower carbonate) unit in the easternmost realms of the Levantine Iberian Range, subdivided in six informal members, even depicting an isopach map for

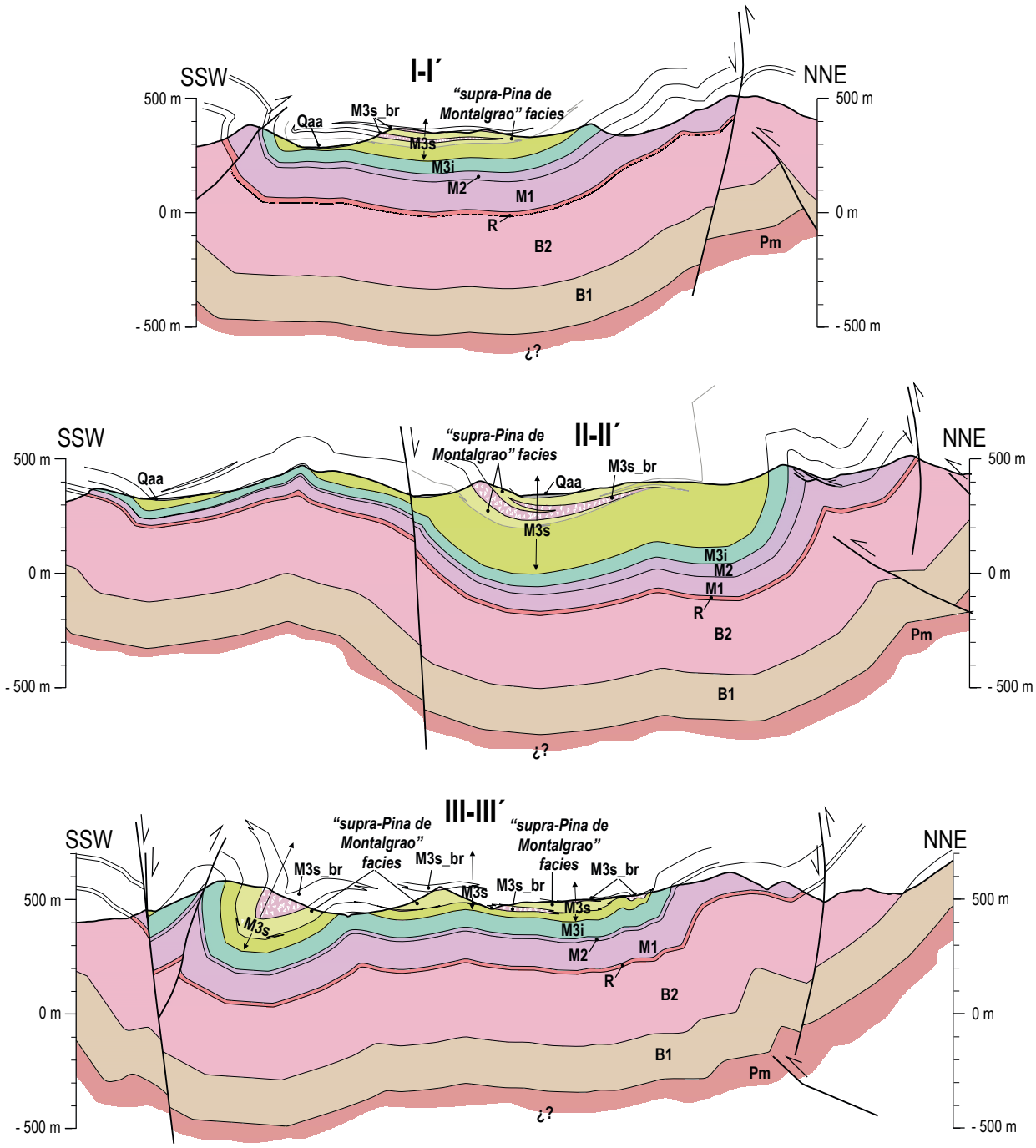

FIGURE 16. Geological cross-sections I-I' to III-III' of the NW sector of the study area (Azuébar-Chóvar sector). See location in Figure 6. Legend as in Figure 3. Vertical and horizontal scales are the same. See explanation in the text.

each member and for the whole unit. Garay (2001) provided 12 lithostratigraphic sections of M1 in the Sierra del Espadán and Sierra Calderona, all of them bounded by the Röt facies at the bottom and by the M2 unit, at the top. In these logs, the thickness of the unit range from 65 to about 110m.

In the light of lithostratigraphic analysis and fossil content of 3 sections in the Manzanera-Alt Palancia and one section near the locality of Serra, Escudero-Mozo *et al.* (2015) concluded that the Muschelkalk carbonate successions in Sierra del Espadán and Sierra Calderona belong entirely to the M3 unit, which in this region they consider to lay directly upon the uppermost Bundsandstein Röt facies. Subsequent works in the same Alt Palancia–Manzanera area, based respectively on detailed geological mapping, palynological dating, and isotope analysis (Ortí *et*

al., 2020), and on lithostratigraphic and sedimentological analysis (Pérez-López *et al.*, 2021), have demonstrated the coexistence of the three Muschelkalk units (M1, M2, and M3) in that region. Similarly, recent geological mapping of the Sierra Calderona confirms the widespread presence of the M1 unit throughout this domain, including the surroundings of Serra (Hernaiz-Huerta, 2022, 2024a).

Escudero-Mozo *et al.* (2015) support their attribution to M3 of the carbonate sections logged on their fossil content. However, some fossils of Anisian age were also recorded in the basal to middle parts of these logs (Escudero-Mozo *et al.*, 2015, fig. 9 therein). In this regard, it is also worth noting that Escudero-Mozo *et al.* (2015) place the contact between the M2 and M3 units below the Anisian–Ladinian boundary (see Fig. 2), thereby assigning the M3 unit to the uppermost part of the Anisian and the entire Ladinian. In contrast, Ortí *et al.* (2020), based on palynological data, position the M2–M3 contact at or slightly above the Anisian–Ladinian boundary (see Fig. 1 and Fig. 4 in this work). In a recent contribution, Márquez-Aliaga *et al.* (2025) have acknowledged that the Serra section of Sierra Calderona entirely corresponds to the M1 unit and dated it as Anisian based on the presence of an exceptional bivalve fauna assemblage, thereby implicity correcting Escudero-Mozo´s interpretation for this area,

The identification of a complete Muschelkalk succession (M1 + M2 + M3) in sierras del Espadán and Calderona not only suggests reconsidering their assignment to the Triassic Levantine-Balearic domain, but also invites a re-evaluation of the interpretation of this region as a paleogeographic high that would have prevented marine incursions during the middle-upper part of the Anisian (Escudero-Mozo *et al.*, 2015; fig. 19 therein).

The "supra-Pina de Montalgrao" facies

Fault control on thickness patterns

The occurrence of thin well-bedded dolostones of the M3i type interbedded within the marly-clayey facies of the "supra-Pina de Montalgrao", has led to their misidentification as the Muschelkalk (M3i) unit and, even, as the Imón Fm Similarly, the "keuperoid" facies, characterized by strong red and yellowish hues, though (usually) lacking gypsum, have been mistakenly assigned to the Keuper in earlier mappings, which originally do not record the significant and distinctive dolostone and breccia packages that are characteristically interbedded within these facies.

The cross-sections depicted in Figure 16 do not exhibit a clear, systematic pattern in the thickening of M3 and "supra-Pina" units (neither in the underlying Muschelkalk or Buntsandstein ones), in part because the basin associated with the syncline has been significantly eroded at its margins, preventing observation of the sedimentary infill's extent to the north or south. In the easternmost section (III-III'), the greatest thickness is recorded in the overturned syncline located to the south, but the evolution of the succession to the north remains unknown due to the lack of infill record. The central section (II-II') is the only one that shows a discernible thickening pattern towards the north in the overall M3s succession (as well as in the underlying Muschelkalk series down to M1). The normal faults affecting the southern sector of the syncline are Neogene in age, as they cut across the entire contractional structure. Consequently, the only faults that may have influenced the sedimentation of the M3s (and some underlying units) are those shown along the northern margin of the syncline, near the southern front of the Sierra del Espadán. These faults are potential normal faults active during the deposition of M3 successions, likely facilitating their thickening towards the north (Fig. 16). These faults were also slightly inverted during Alpine compression.

Tectonically induced versus dissolution breccias

The abundant and, in most cases, thick (>10-20m) intercalations of breccia packages may be interpreted as a primary evidence of tectonic instabilities concurrent with the deposition of the "supra-Pina de Montalgrao" facies. As previously discussed, the "keuperoid" facies that host these breccias frequently exhibit breccia-like textures at the matrix scale or contain substantial levels of microbreccias of the same dolomitic composition as the larger breccia clasts. The formation of these breccias by fragmentation of brittle "M3i type" thin well-bedded dolostone packages interbedded within the "keuperoid" marly-clayey facies can be observed in several outcrops (*e.g.* Fig. 12). Thick packages composed solely of dolomitic or calcareous-dolomitic breccias formed by decimeter- to meter-sized blocks occur in other outcrops (*e.g.* Figs. 10G; 15F).

In addition to the presence of breccias, other aspects also suggest a degree of tectonic control: i) the evidence of syn-sedimentary deformation described in previous sections; ii) the distinct localization of the depositional basin of these "supra-Pina de Montalgrao" facies in the Azuebar-Chóvar area, likely influenced by syn-sedimentary faults (now associated with the inverted southern front of the Sierra Calderona), which may have facilitated the greater accumulation of these facies and, more broadly, of the entire Muschelkalk sequence as well as other underlying units and iii) the appearance of breccias within the basin is also accompanied by a marked and sudden siliciclastic input in the basin, likely derived from nearby uplifted areas undergoing denudation.

Taken together, these features allow interpreting the breccias as possible tectofacies associated with late reactivations of the Permo-Triassic mechanical extension phase. These reactivations likely triggered gravitational instability and the partial disintegration of M3i-type carbonate platforms.

Pérez-López and Pérez-Valera (2021) described soft-sediment deformation structures within the Muschelkalk, the Keuper, and the Zamoranos Fm (equivalent to the Imón Fm) in the External Zones of the Betic Cordillera, drawing comparisons with analogous features reported in the Triassic successions of Europe (*e.g.* Basilone *et al.*, 2016; Chatalov, 2017; Föhlisch and Voigt, 2001; Matysik and Szulc, 2019; Knaust, 2000, 2002, among others). These structures include slumps, breccias, debrites, and seismites, coexisting with local unconformities, synsedimentary faults, and contemporaneous volcanism, which these authors interpret as evidence of rifting concurrent with the deposition of the mentioned units. However, none of these soft-sediment deformation structures, nor the associated breccias and debrites, exhibit the volume, outcrop extent, or representativeness of the breccias included within the "supra-Pina de Montalgrao" facies described in the present study.

On the other hand, the brecciation of carbonate horizons resulting from the dissolution of stratigraphically associated evaporitic deposits—producing so-called solution-collapse breccias—has been extensively documented (Flude *et al.*, 2025; Friedman, 1997; Stanton, 1966; Warren, 2016). Notable examples have been reported in Triassic formations across Europe (*e.g.* Karakitsios and Pomoni, 1998; Pomoni-Papaionou and Karakitsios, 2002), as well as in Triassic units from other regions (*e.g.* Ackermann *et al.*, 1995), and in formations of varying ages that share sedimentary and tectonic contexts comparable to the present study area (*e.g.* Eliassen and Talbot, 2005; Swennen *et al.*, 1990). Particularly pertinent for comparison with the calcareous-dolomitic breccia packages intercalated within the "keuperoid" facies are instances of solution breccias occurring as continuous, stratiform levels within their host formations (Ackermann *et al.*, 1995; Eliassen and Talbot, 2005; Swennen *et al.*, 1990).

These stratiform solution breccias typically exhibit sharply defined basal contacts, irregular but well-delimited upper boundaries, a downwards increase in brecciation intensity, and the presence of insoluble residues derived from interbedded evaporitic layers. However, assessing the presence of these diagnostic features in the study area is hindered by the generally poor exposure of breccia´s packages boundaries. A particularly challenging aspect is the general absence of recognizable evaporitic deposits within the "keuperoid" facies. It is possible, however, that such deposits were originally present but subsequently removed through groundwater dissolution, as proposed by Ackermann *et al.* (1995) for the Late Triassic Lower Blomidon Fm in the Fundy rift basin, Nova Scotia.

Support for a dissolution-related brecciation origin may include the extreme angularity of fragments and blocks, visible even in the matrix, within some breccia bodies, suggesting in situ formation without transport, as well as their frequent association to carniolar lithologies (evaporite solution-related textures). Nonetheless, it is important to acknowledge that in situ brittle deformation of dolostones may produce similar results. In certain well-exposed outcrops of calcareous-dolomitic breccias, particularly those observed in quarries, potential collapse structures or chimney-like features with a V-shaped geometry can be inferred. Although detailed sedimentological studies are still lacking, these preliminary observations suggest that some of these breccias might plausibly be classified as solution-collapse breccias.

The stratigraphic assignment of the "supra-Pina de Montalgrao" facies

In the literature related to the Triassic of the Iberian Peninsula and the Balearic Islands (*e.g.* Gibbons and Moreno, 2002; Quesada and Oliveira, 2019; Vera, 2004), there is no reference to facies resembling, even remotely, those identified in this study as "supra-Pina de Montalgrao". Likewise, such facies are absent from the European literature addressing the uppermost deposits of the Muschelkalk and their transition to the Keuper within the Germanic Triassic Basin (*e.g.* Pérez-López *et al.*, 2020, and references therein), as well as from studies focusing on syn-sedimentary deformation structures associated with this interval (*e.g.* Pérez-López and Pérez-Valera, 2021, and references therein).

The term "supra-Pina de Montalgrao" facies (or "supra-Pina de Montalgrao unit") as employed in this study refers to the massive marly-clayey "keuperoid" facies that encompass intercalated, well-bedded dolostone and breccia packages, as previously described. This designation reflects not only the unequivocal stratigraphic position of these facies above the Pina de Montalgrao Fm, but also the gradational and lateral transitions observed between the two units. The lithological assemblages within these facies suggest recurrent depositional environments analogous to those described for the underlying M3i and M3s units. In the case of "supra-Pina de Montalgrao" facies, with prevalence of restricted lagoon/sabkha-type coastal environments, rather than shallow carbonate platforms, within a context of significant tectonic instability, quite probably driven by late-stage rifting reactivations.

An interesting parallel to the "supra-Pina de Montalgrao" facies described in this study is found in the upper Muschelkalk-Keuper transitional succession of the Serra de Prades (northeastern Spain), as documented by De Santisteban and Taberner (1987). In that region, the authors identified in the uppermost part of the Muschelkalk M3 interval a ≈40m thick dolomitic succession characterized by abundant sabkha-type evaporitic features, particularly pseudomorphs of anhydrite and gypsum preserved as dolomite. This unit records a gradual shift from subtidal to intertidal and supratidal depositional environments, with numerous indicators of shallow evaporitic settings, including nodular anhydrite replaced by dolomite, chicken-wire fabrics, tepee structures, and polygonal crack systems. Collectively, these deposits represent a phase of lagoonal to supratidal sedimentation that bears a close resemblance to that inferred for the uppermost Muschelkalk "supra-Pina de Montalgrao" facies described in the present study area.

An alternative interpretation is to consider the possibility of assigning these facies to the Keuper, given their apparent lithological affinities—particularly the "keuperoid" character that prompted the informal designation used herein. However, Keuper outcrops within the study area are scarce and consistently limited to thin, discontinuous soles preserved at the base of the isolated patches of Jurassic units (Figs. 3; 14). These occurrences are typically composed almost exclusively of reddish, purplish, and whitish clays, occasionally interbedded with thin gypsum layers or discontinuous bodies of massive gypsum (Figs. 17; 19). Notably, these outcrops lack both the breccia and the dolostone intervals characteristic of the "supra-Pina de Montalgrao" facies. The Keuper is found underlying different Jurassic formations (*e.g.* Figs. 14; 18), with contacts that may represent either a low-angle subtractive contact (detachment) or, perhaps, the effects of salt tectonics. In these cases, the basal contact with the underlying units is rarely exposed, owing to the incompetent nature of both the Keuper and the subjacent facies, but geological mapping consistently reveals the Keuper overlying the "supra-Pina de Montalgrao" facies, which constitutes the uppermost part of the Muschelkalk succession (Figs. 3; 14; 18).

Consequently, considering its stratigraphic position and the absence of diagnostic Keuper lithologies, it appears more reasonable to assign the "supra-Pina de Montalgrao" unit to the uppermost Muschelkalk rather than to the Keuper. From a paleogeographic perspective, this interpretation suggests that the semi-arid climatic conditions characteristic of the Keuper sedimentary environment could have begun to establish in the study area earlier, possibly in the late Ladinian, alternating with last, ephemeral episodes of shallow carbonate platform deposition.

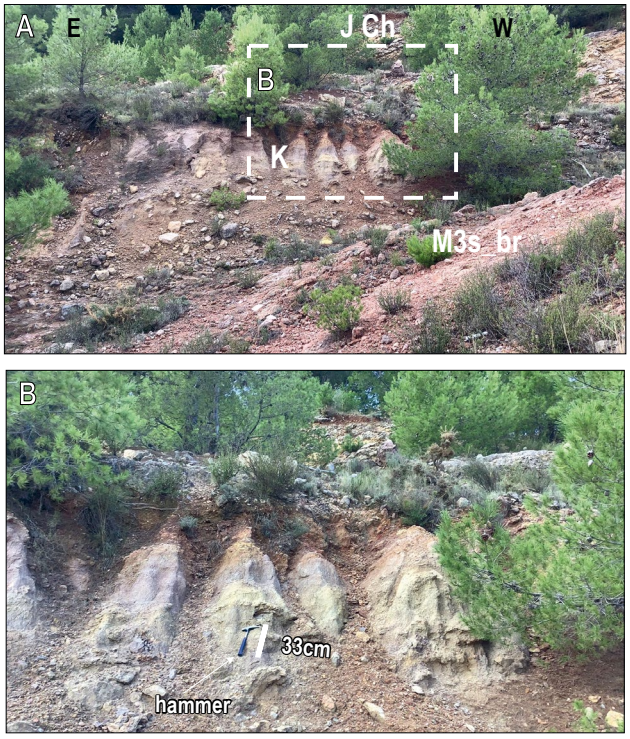

FIGURE 17. Keuper (K) outcrop close to La Pedrera quarry (point 3 in Fig. 14). The stratigraphic position of this outcrop in La Pedrera section is indicated in Figure 15. This Keuper overlies "supra-Pina de Montalgrao" "keuperoid" facies with breccias (M3s_br) situated in stratigraphic, upward continuity with the mega-breccia exposed in the southern quarry front shown in Figure 15. The contact between these two units (K and "keuperoid" facies), possibly faulted, is not visible due to soil cover. The Keuper (K) is overlain by a succession of well-bedded, slightly undulating limestones, belonging to the lower part of the Casinos Fm of the Chelva Group (JCh). This is a subtractive contact, interpreted as a low-angle fault or detachment in the map (Figure 14). See hammer for scale (33cm) in the lower photograph.

For its definitive stratigraphic assignment to the uppermost part of the M3, to the Keuper, or potentially to another stratigraphic interval, additional studies will be necessary. These may include palynological dating and/or isotopic correlations of oxygen ($\delta^{18}O$) and sulfur ($\delta^{34}S$) in sulfate-bearing rocks, as conducted by Ortí *et al.* (2020, 2022, 2025) across all the marly-clayey formations in the region. Nevertheless, it is imperative that these analyses be performed on samples obtained from units with clearly defined stratigraphic positions. This will necessitate a comprehensive revision of the regional geological mapping.

CONCLUSIONS

The results of this study indicate that the Muschelkalk M2 unit is present throughout the investigated sector of the Sierra del Espadán, including the easternmost outcrops close to the coast. Nevertheless, due to its reduced thickness, the unit may locally wedge out or be entirely

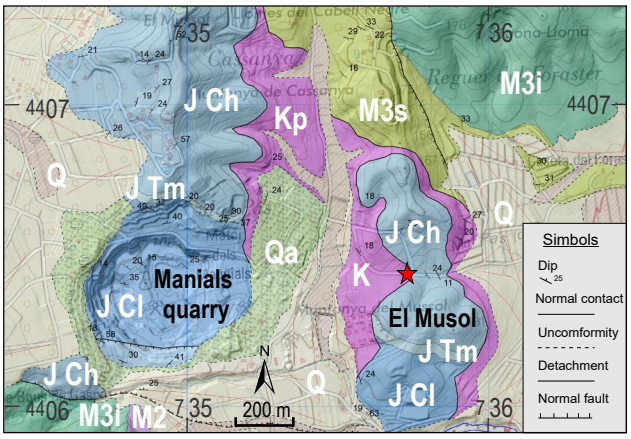

FIGURE 18. Geological map of the El Musol area (near the Manials quarry) enlarged from Figure 3. The map shows the Keuper (K) overlying the M3s unit. Several tens of meters of the Pina de Montalgrao Fm can be clearly recognized overlying the M3i unit, being the contact between these two units partially faulted. In the uppermost part of the M3s outcrop, remnants of "supra-Pina de Montalgrao" "keuperoid" facies with discontinuous intervals of dolomitic breccias (not represented in the map) are present. The contact between these facies and the Keuper is not visible, as it is covered by colluvium. Legend as in Figure 3, except for: JCl, Fm Cuevas Labradas (Lower Jurassic); JTm, Fm Turmiel (Lower Jurassic); JCh, Chelva Group (Middle Jurassic). The red star indicates the location of the pictures shown in Figure 19.

absent, producing continuous dolomitic successions composed of M1+M3 carbonates. This pattern supports the interpretation that the Triassic succession in this region is more closely related to the Mediterranean type, rather than to the Levantine-Balearic one.

The carbonate M1 unit consistently outcrops in stratigraphic continuity with the Röt facies capping the Buntsandstein B2 succession. Therefore, previous proposals that attributed the entire Muschelkalk carbonate succession of these domains to the M3 unit should be reconsidered.

Above the M3 succession, the newly identified 'supra-Pina de Montalgrao' facies are characterized by thick marly-clayey successions with intercalated thin-bedded dolostones and abundant dolomitic breccias. However, their depositional origin and precise stratigraphic assignment remain uncertain. These facies may reflect tectonic instability related to late reactivations of Permo-Triassic rifting, but the alternative possibility of solution-collapse breccias linked to evaporite dissolution cannot be excluded. To clarify these questions, complementary studies are needed, including detailed sedimentological analysis, isotopic correlations, and especially, palaeontological dating.

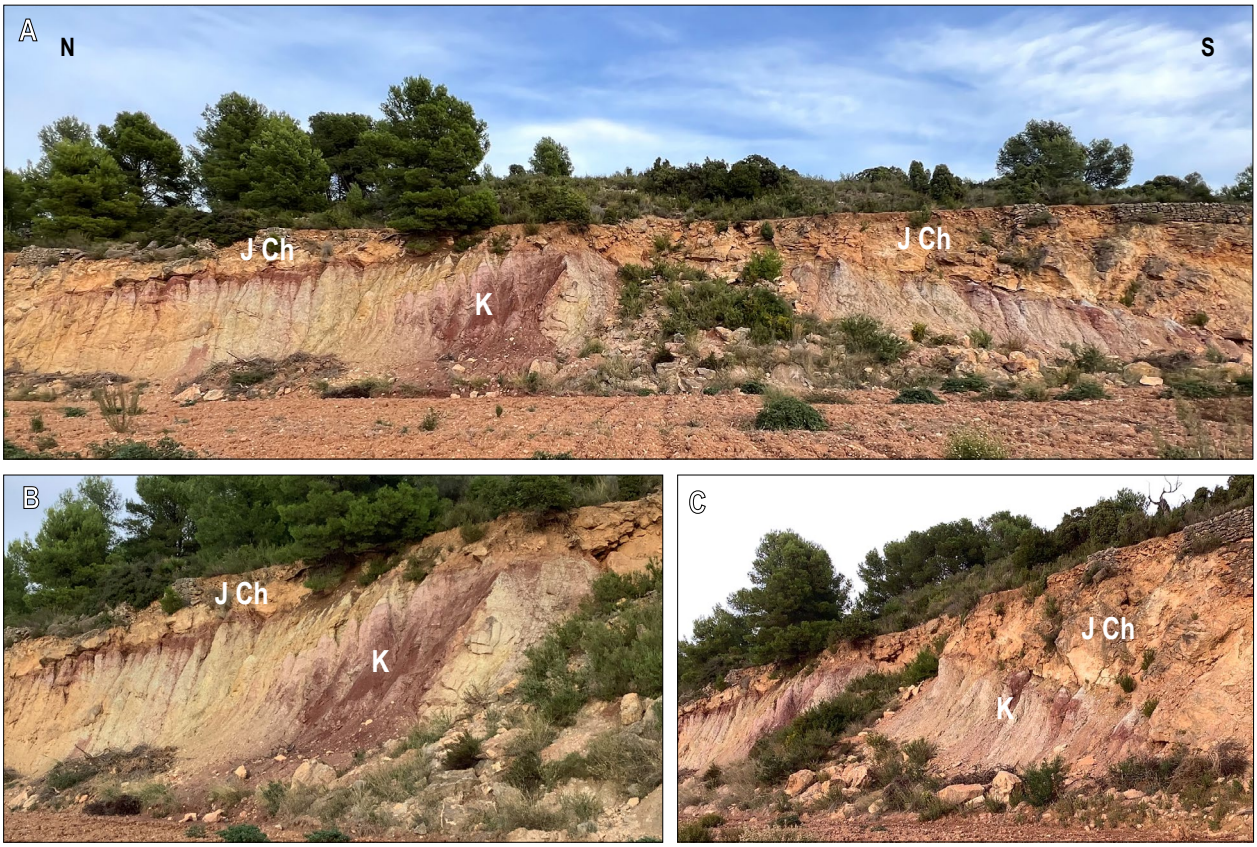

FIGURE 19. Keuper (K) outcrops in the El Musol area. See location in Figure 18. At this point, the Keuper is overlain by the limestones of the Casinos Fm of the Chelva Group (JCh), and farther south, by the marls and marly limestones of the Turmiel Fm, and the well bedded limestone succession of Cuevas Labradas Fm (see map in Figure 18). This represents a subtractive contact interpreted as a low-angle fault or detachment.

Resolving the presence, stratigraphic position, and nature of the M2 unit and the 'supra-Pina de Montalgrao' facies is of major significance, since they bear important palaeogeographic implications. Their recognition in this sector of the Iberian Range may affect the interpretation of marine connections, subsidence patterns, and palaeogeographic reconstructions of the western Tethys during the Middle to Late Triassic. These implications should be tested against evidence from other regions through integrated multidisciplinary studies.

ACKNOWLEDGMENTS

The geological mapping of the La Vall d´Uixó 1:25,000 scale sheet (No 668-II) was funded by the CN IGME_CSIC (Spanish Geological Survey) internal project No. 2938 in the context of the agreement signed with the Institut Cartogràfic Valencià for the "*Development of a digital continuous geological map of a coastal sector of the Valencia Authonomous Community at 1:25,000 scale*". The authors are grateful to both institutions for the facilities given to publish this work. Further mapping has been funded by the CN IGME_CSIC internal competitive project TECTOCALESPA (3164) and the AEI (MICINN) REVISEBETICS project (PID2020-119651RB-I00/AEI/10.13039/501100011033). A. Ramos work was funded by the European Social Fund Plus and the Generalitat Valenciana project "Cenozoic extensional tectonics in the SW margin of the Valencian Trough" (CIAPOS/2022/082). Pictures shown in Figures 8A, 15A, B, were taken by Albert Maymó with the aid of a dron. Constructive suggestions from Gabriel Cofrade and another anonymous reviewer improved the final version of the manuscript.

REFERENCES

Ackermann, R.V., Schlische, P.W., Olsen, P.E., 1995. Synsedimentary collapse of portions of the Lower Blomidon Formation (Late Triassic), Fundy Rift Basin, Nova Scotia. Canadian Journal of Earth Sciences, 32, 1965-1976. DOI: https://doi.org/10.1139/e95-150

Álvaro, M., Capote, R., Vegas, R., 1979. Un modelo de evolución geotectónica para la Cadena Celtibérica. Acta Geológica Hispánica, 14, 172-177.

Basilone, L., Sulli, A., Morticelli, M.G., 2016. The relationships between soft-sediment deformation structures and synsedimentary extensional tectonics in Upper Triassic deep-water carbonate succession (Southern Tethyan rifted continental margin—Central Sicily). Sedimentary Geology, 344, 310-322. DOI: https://doi.org/10.1016/j.sedgeo.2016.01.010

Chatalov, A., 2017. Anachronistic and unusual carbonate facies in uppermost Lower Triassic rocks of the western Balkanides, Bulgaria. Facies, 63, 24. DOI: https://doi.org/10.1007/s10347-017-0505-0

De La Horra, R., Arche, A., López-Gómez, J., Sopeña, A., Sánchez-Moya, Y., Barrenechea, J.F., Galán-Abellán, B., Borruel-Abadía, V., Vargas, H., 2019. Tectonics and sedimentation during the beginning of the - Permo- Triassic - basin. In: Quesada, C., Oliveira, J.T. (eds.). The Geology of Iberia. A geodynamic approach. Volume 3: The Alpine Cycle. Springer Nature, Regional Geology Reviews, 69-73.

De Santisteban, C., Taberner, C., 1987. Depósitos evaporíticos de ambiente sabkha preservados como psudomorfos en dolomita, en los materiales superiores de las facies Muschelkalk de la Serra de Prades (Tarragona). Cuadernos de Geología Ibérica, 11, 199-214.

De Vicente, G., Vegas, R., Muñoz-Martín, A., Van Wees, J.D., Casas-Sainz, A., Sopeña, A., Sánchez-Moya, Y., Arche, A., López-Gómez, J., Olaiz, A., Fernández-Lozano, J., 2009. Oblique strain partitioning and transpression on an inverted rift: The Castilian branch of the Iberian chain. Tectonophysics, 470(3-4), 224-242. DOI: https://doi.org/10.1016/j.tecto.2008.11.003

De Vicente, G., Casas-Sainz, A., Vegas, R., 2019. The Iberian chain and the Catalan coastal ranges. In: Quesada, C., Oliveira, J.T. (eds.). The Geology of Iberia. A geodynamic approach. Volume 3: The Alpine Cycle. Springer Nature, Regional Geology Reviews, 512-517.

Doubinger, J., López-Gómez, J., Arche, A., 1990. Pollen and spores from the Permian and Triassic sediments of the southeastern Iberian Ranges, Cueva del Hierro (Cuenca) to Chelva-Manzanera (Valencia-Teruel) region, Spain. Review of Palaeobotany and Palynology, 66, 25-45. DOI: https://doi.org/10.1016/0034-6667(90)90027-G

Eliassen, A., Talbot, M.R., 2005. Solution-collapse breccias of the Minkinfjellet and Wordiekammen Formations, Central Spitsbergen, Svalbard: a large gypsum palaeokarst system. Sedimentology, 52, 775-794. DOI: https://doi.org/10.1111/j.1365-3091.2005.00731.x

Escudero-Mozo, M.J., Márquez-Aliaga, A., Goy, A., Martín-Chivelet, J., López-Gómez, J., Márquez, L., Arche, A., Plasencia, P., Pla, C., Sánchez-Fernández, D., 2015. Middle Triassic carbonate platforms in eastern Iberia: Evolution of their fauna and palaeogeographic significance in the western Tethys. Palaeogeography, Palaeoclimatology, Palaeoecology, 417, 236-260. DOI: https://doi.org/10.1016/j.palaeo.2014.10.041

Escudero-Mozo, M.J., Martín-Chivelet, J., López-Gómez, J., Arche, A., Márquez-Aliaga, A., Goy, A., Márquez, L., Plasencia, P., Sánchez- Fernández, D., 2019. The Middle Triassic Carbonate Ramps (Muschelkalk) in the Iberian Basin. In: Quesada, C., Oliveira, J.T. (eds.). The Geology of Iberia. A geodynamic approach. Volume 3: The Alpine Cycle. Springer Nature, Regional Geology Reviews, 74-75.

Flude, S., Bond C.E., Butler, R.W.H., 2025. Are geological description practices and classification schemes fit for future use? Breccias as an example, Earth-Science Reviews, 266, 105140. DOI: https://doi.org/10.1016/j.earscirev.2025.105140

Föhlisch, K., Voigt, T., 2001. Synsedimentary deformation in the Lower Muschelkalk of the Germanic Basin. In: McCaffrey,

W.D., Kneller, B.C., Peakall, J. (eds.). Particulate Gravity Currents. Special Publications International Association of Sedimentologists, 31, 279-297.

Fontboté, J.M., Guimerá, J., Roca, E., Sabat, F, Santanach, P., Fernández-Ortigosa, F., 1990. The Cenozoic geodynamic evolution of the Valencia trough (western Mediterranean). Revista de la Sociedad Geológica de España, 3, 249-259.

Friedman, G.M., 1997. Dissolution-collapse breccias and paleokarst resulting from dissolution of evaporite rocks, especially sulfates. Carbonates and Evaporites, 12, 53-63. DOI: https://doi.org/10.1007/BF03175802

Garay, P., 2001. El dominio triásico Espadán-Calderona. Contribución a su conocimiento geológico e hidrogeológico. PhD. Thesis. Universidad de Valencia, 692pp

Gibbons, W., Moreno, T., 2002. The Geology of Spain. Regional Geology and Guide Books. London, The Geological Society, 649pp.

Gómez, J.J., 2019a. The Evolution of Eastern Iberia During the Early Stages of the Alpine Cycle in the Context of the Atlantic and Tethys Oceans Plate Tectonics. In: Quesada, C., Oliveira, J.T. (eds.). The Geology of Iberia. A geodynamic approach. Volume 3: The Alpine Cycle. Springer Nature, Regional Geology Reviews, 15-18.

Gómez, J.J., 2019b. The Onset of the Passive Margin Stage and the Triassic–Jurassic Boundary in Northern and Eastern Iberia. In: Quesada, C., Oliveira, J.T. (eds.). The Geology of Iberia. A geodynamic approach. Volume 3: The Alpine Cycle. Springer Nature, Regional Geology Reviews, 115-121.

Guimerà, J., Álvaro, M., 1990. Structure et évolution de la compression alpine dans la Chaîne ibérique et la Chaîne côtiere catalane (Espagne). Bulletin de la Société Géologique de France, 6, 339-348. DOI: https://doi.org/10.2113/gssgfbull.VI.2.339

Gutiérrez Elorza, M., Pedraza Gilsanz, J., 1973. Mapa Geológico de España a escala 1:50.000, 2ª Serie y Memoria explicativa de la Hoja de Segorbe (Nº 640). Instituto Geológico y Minero de España (IGME).

Hernaiz-Huerta, P.P., 2022. La estructura de Sierra Calderona (SE de la C. Ibérica): El colapso extensional neógeno de un edificio Permo-Triásico y Jurásico estratigráficamente complejo. Madrid, Guía de campo de la XXXIII Reunión de la Comisión de Tectónica, Sociedad Geológica de España(SGE), Website: https://sge.usal.es/comisiones/memorias_tectonica/memoria_33.pdf

Hernaiz-Huerta, P.P., 2023. Mapa geológico a escala 1:25.000 de la hoja de La Vall d´Uixó (668 II). In: Institut Cartogràfic Valencià-Centro Nacional Instituto Geológico y Minero de España_Consejo Superior de Investigaciones Científicas (ICV_CN IGME) (eds.). Proyecto de actualización de la Cartografía Geológica a escala 1:25k en el ámbito litoral de la Comunidad Valenciana.Website: https://icv.gva.es/va/geocv25

Hernaiz-Huerta, P.P., 2024a. The geology of Sierra Calderona (SE Iberian Cordillera, Spain), a review. Results of a new 1:25.000 scale geological mapping. Journal of Maps, 20(1), 2302363. DOI: https://doi.org/10.1080/17445647.2024.2302363

Hernaiz-Huerta, P.P., 2024b. Nota sobre las peculiaridades estratigráficas del Muschelkalk en el sector de La Vall d´Uixó (Sierra del Espadán, Cordillera Ibérica). In: Ruiz-Costán, A., Martín-Lechado, C., Pedrera-Parias, A. (eds.). Contribuciones al XI Congreso Geológico de España. Geotemas, 20, 127-130.

Hernaiz-Huerta, P.P., Ollé López, M., Masana Closa, E., Perea Manera, H., 2024c. Resultados de una nueva cartografía geológica de la falla de La Vall d´Uixó (Sierra del Espadán, Cordillera Ibérica). In: Ruiz-Costán, A., Martín-Lechado, C., Pedrera-Parias, A. (eds.). Contribuciones al XI Congreso Geológico de España. Geotemas, 20, 784-787.

Hernández, A., Anadón, P., Gabaldón, V. (and collaborators), 1985a. Mapa Geológico de España a escala 1:200.000, 2ª Serie, y Memoria explicativa de la Hoja de Llíria (Nº 55). Instituto Geológico y Minero de España (IGME).

Hernández, A., Anadón, P., Gabaldón, V. (and collaborators), 1985b. Mapa Geológico de España a escala 1:200.000, 2ª Serie, y Memoria explicativa de la Hoja de Valencia (Nº 56). Instituto Geológico y Minero de España (IGME).

IGME/LNEG (Instituto Geológico y Minero de España/Laboratório Nacional de Energía e Geología), 2015. Mapa Geológico de la Península Ibérica, Baleares y Canarias a escala 1:1.000.000. Madrid, Instituto Geológico y Minero de España (IGME). Website: https://info.igme.es/cartografiadigital/geologica/Geologicos1MMapa.aspx?Id=Geologico1000_(2015)

Karakitsios, V., Pomoni-Papaioannou, F., 1998. Sedimentological study of the Triassic solution-collapse breccias of the Ionian Zone (NW Greece). Carbonates Evaporites, 13, 207-218. DOI: https://doi.org/10.1007/BF03176594

Knaust, D., 2000. Signatures of tectonically controlled sedimentation in Lower Muschelkalk carbonates (Middle Triassic) of the Germanic basin. In: Bachmann, G.H., Lerche, I. (eds.). Epicontinental Triassic International Symposium. Zentralblatt für Geologie und Paläontologie, Volume 1, 893-924.

Knaust, D., 2002. Pinch-and-swell structures at the Middle/Upper Muschelkalk boundary (Triassic): evidence of earthquake effects (seismites) in the Germanic Basin. International Journal of Earth Sciences, 91, 291-303. DOI: https://doi.org/10.1007/s005310100225

Liesa, C., Soria, A.R., Casas, A., Aurell, M., Meléndez, N., Bádenas, B., Fregenal-Martínez, M., Navarrete, R., Peropadre, C., Rodríguez-López, J.P., 2019. The Late Jurassic–Early Cretaceous rifting. The South-Iberian, Central-Iberian and Maestrazgo basins. In: Quesada, C., Oliveira, J.T. (eds.). The Geology of Iberia. A geodynamic approach. Volume 3: The Alpine Cycle. Springer Nature, Regional Geology Reviews, 214-228.

López-Gómez, J., Arche, A., 1986. Estratigrafía del Pérmico y Triásico en facies Buntsandstein y Muschelkalk en el sector SE de la Rama Castellana de la Cordillera Ibérica (prov. de Cuenca y Valencia). Estudios Geológicos, 42, 259-270.

López-Gómez, J., Arche, A., 1992. Las unidades litoestratigráficas del Pérmico y Triásico inferior y medio en el sector SE de

la Cordillera Ibérica. Estudios Geológicos, 48(3-4), 123-143. DOI: https://doi.org/10.3989/ egeol.92483-4376

López-Gómez, J., Arche, A., Calvet, F., Goy, A., 1998. Epicontinental marine carbonate sediments of the Middle and Upper Triassic in the westernmost part of the Tethys Sea, Iberian Peninsula. Zentralblatt für Geologie und Paläontologie, 9-10, 1033-1084.

Márquez-Aliaga, A., Ros-Franch, S., Stori, L., Escudero-Mozo, M.J., López-Gómez, J., Martín-Chivelet, J., 2025. Anisian bivalves from Serra (Valencia, Iberian Ranges): taxonomy, environments and biogeographic implications. Journal of Iberian Geology DOI: https://doi.org/10.1007/s41513-025-00309-6

Matysik, M., Szulc, J., 2019. Shallow-marine carbonate sedimentation in a tectonically mobile basin, the Muschelkalk (Middle Triassic) of Upper Silesia (southern Poland). Marine and Petroleum Geology, 107, 99-115. DOI: https://doi.org/10.1016/j.marpetgeo.2019.05.016

Ortí, F., Pérez-López, A., Salvany, J.M., 2017. Triassic evaporites of Iberia: sedimentological and palaeogeographical implications for the western Neotethys evolution during the Middle Triassic–Earliest Jurassic. Palaeogeography, Palaeoclimatology, Palaeoecology, 47, 157180. DOI: https://doi.org/10.1016/j.palaeo.2017.01.025

Ortí, F., Pérez-López, A., 2019. Permian-Triassic Rifting Stage. The Iberian Basin. Evolution of the Keuper Evaporites. In: Quesada, C., Oliveira, J.T. (eds.). The Geology of Iberia. A geodynamic approach. Volume 3: The Alpine Cycle. Springer Nature, Regional Geology Reviews, 75-78.

Ortí, F., Guimerà, J., Götz, A., 2020. Middle-Upper triassic stratigraphy and structure in the Alt Palància region (eastern Iberian Chain): A multidisciplinary approach. Geologica Acta, 18(4), 1-26. DOI: https://doi.org/10.1344/GeologicaActa2020.18.4

Ortí, F., Pérez-López, A., Pérez-Valera, F., Benedicto, C., 2022. Isotope composition ($\delta^{34}S$, $\delta^{18}O$) of the Middle Triassic-Early Jurassic sulfates in eastern Iberia. Sedimentary Geology, 431, 106104. DOI: https://doi.org/10.1016/j.sedgeo.2022.106104

Ortí, F., Pérez-López, A., García-Ávila, M., Benedicto, C., Garay-Martín, P., Díez, J.B., 2025. Middle Muschelkalk Facies in the Vlencian sector of the Triassic Iberian Basin: implications for the paleogeographic evolution of the central-eastern Iberian Platform. Journal of Iberian Geology. DOI: https://doi.org/10.1007/s41513-025-00310-z

Pérez-Arlucea, M., Sopeña, A., 1985. Estratigrafia del Pérmico y Triásico en el sector central de la rama castellana de la Cordillera Ibérica. Estudios Geológicos, 41, 207-222.

Pérez-López, A., Pérez-Valera, F., 2007. Palaeogeography, facies and nomenclature of the Triassic units in the different domains of the Betic Cordillera (S Spain). Palaeogeography, Palaeoclimatology, Palaeoecology, 254, 606-626. DOI: https://doi.org/10.1016/j. palaeo.2007.07.012

Pérez-López, A., Pérez-Valera, F., 2021. Tectonic signatures in the Triassic sediments of the Betic External Zone (southern Spain) as possible evidence of rifting related to the Pangaea breakup. Comptes Rendus Géoscience, 353, 355-376. DOI: 10.5802/crgeos.85

Pérez-López, A., Martín-Algarra, A., Pérez-Valera, F., Pérez-Valera, J.A., Viseras C., 2019. The Betic Basin. From Initial to Mature Rifting Phases. In: Quesada, C., Oliveira, J.T. (eds.). The Geology of Iberia. A geodynamic approach. Volume 3: The Alpine Cycle. Springer Nature, Regional Geology Reviews, 90-91.

Pérez-López, A., Benedicto, C., Ortí, F., 2021. Middle Triassic carbonates of Eastern Iberia (Western Tethyan Realm): A shallow platform model. Sedimentary Geology, 420, 105904. DOI: https://doi.org/10.1016/j.sedgeo.2021.105904

Pérez-Valera, F., Pérez-López, A., Götz, A.E., Ros-Franch, S., Márquez-Aliaga, A., Baeza-Carratalá, J.B., Pérez-Valera, J.A., 2023. First record of Anisian deposits in the Betic External Zone of southern Spain and its paleogeographical implications. Sedimentary Geology, 449, 106374. DOI: https://doi.org/10.1016/j.sedgeo.2023.106374

Pomoni-Papaioannou, F., Karakitsios, V., 2002. Facies analysis of the Trypali carbonate unit (Upper Triassic) in central-western Crete (Greece): an evaporite formation transformed into solution-collapse breccias. Sedimentology, 49, 1113-1132. DOI: https://doi.org/10.1046/j.1365-3091.2002.00480.x

Quesada, C., Oliveira, J.T. (eds.), 2019. The Geology of Iberia, A Geodynamic Approach. Volume 3: The Alpine Cycle. Springer Nature, Regional Geology Reviews, 566pp.

Salvany, J.M., 1990. Introducción a las evaporitas triásicas de las cadenas periféricas de la cuenca del Ebro: Catalanides, Pirineo y Región Cantábrica. In: Ortí, F., Salvany, J.M. (eds.). Formaciones evaporíticas de la Cuenca del Ebro y cadenas periféricas, y de la Zona de Levante. ENRESA-Universitat de Barcelona, 9-20.

Sánchez Moya, Y., Sopeña, A., 2004. El Rift Mesozoico Ibérico. In: Vera, J.A. (ed.). Geología de España. Sociedad Geológica de España-Instituto Geológico y Minero de España (SGE-IGME), 484-495.

Simón, J.L., 2004. La tectónica extensional neógena-cuaternaria en la Cordillera Ibérica. In: Vera, J.A. (ed.). Geología de España. Sociedad Geológica de España-Instituto Geológico y Minero de España (SGE-IGME), 615-617.

Sopeña, A., López-Gómez, J., Arche, A., Pérez-Arlucea, M., Ramos, A., Virgili, C., Hernando, S., 1988. Permian and Triassic basins of the Iberian península. In: Manspeizer, W. (ed.). Triassic-Jurassic Rifting. Continental Breakup and the Origin of the Atlantic Ocean and Passive margins, Part B. Developments in Geotectonics, 22, 758-785. DOI: https://doi.org/10.1016/B978-0-444-42903-2.50036-1

Stanton, R.J.Jr., 1966. The solution brecciation process. Geological Society of America Bulletin, 77, 843-847.

Swennen, R., Viaene, W., Cornelissen, C., 1990. Petrography and geochemistry of the Belle Roche breccia (lower Visean, Belgium): evidence for brecciation by evaporite dissolution. Sedimentology, 37, 859-878. DOI: https://doi.org/10.1111/j.1365-3091.1990.tb01830.x

Tucker, M.E., 1982. The Field Description of Sedimentary Rocks. Geological Society Handbooks, 48pp.

Vegas, R., 1992. The Valencia Trough and the origin of the Western Mediterranean basins. Tectonophysics, 203(1-4), 249-261. DOI: https://doi.org/10.1016/0040-1951(92)90226-V

Vera, J.A. (ed.), 2004. Geología de España. Sociedad Geológica de España-Instituto Geológico y Minero de España (SGE-IGME), 884pp.

Virgili, C., Sopeña, A., Ramos, A., Hernando, S., 1977. Problemas de la cronoestratigrafía del Trías en España. Cuadernos de Geología Ibérica, 4, 57-88.

Warren, J.K., 2016. Salt Dissolution and Pointers to Vanished Evaporites: Karst, Breccia, Nodules and Cement. In: Warren, J.K. (ed.). Evaporites. Springer International Publishing, 613-761. DOI: https://doi.org/10.1007/978-3-319-13512-0_7

Ziegler, P.A., 1982. Geological Atlas of Western and Central Europe. Shell International Petroleum Maatschappij, B.V. Elsevier Scientific Publishing Company, 130pp. DOI: 10.1017/s0016756800029344

Ziegler, P.A., 1988. Evolution of the Arctic-North Atlantic and the Western Tethys. American Association of Petroleum Geologists (AAPG), Memoir 43, 198p. DOI: https://doi.org/10.1306/M43478

Manuscript received June 2025;
revision accepted October 2025;
published Online January 2026.